

Supporting Information for

First and Second Sphere Interactions Accelerate Non-Native *N*-Alkylation Catalysis by the Thermostable, Methanol-Tolerant B₁₂-Dependent Enzyme MtaC

Amardeep Kumar,¹ Xinhang Yang,^{1,‡} Jianbin Li,¹ Jared C. Lewis^{1,*}

¹Department of Chemistry, Indiana University, Bloomington, IN 47405, USA

[‡]Current address: Enzymaster Bio-Engineering Co., Ltd., 333 North Century Avenue, Ningbo, China

*jcl3@iu.edu

Table of Contents

I. Supplementary Figures	2
II. Materials and Instruments	5
A) Materials	5
B) Instruments	5
C) Software	6
III. Enzyme Preparation	6
A) CarH Homologue Identification	6
B) Enzyme gene preparation	6
C) Protein Preparation	9
IV. Bioconversion Protocol and Analysis	10
A) Reaction Optimization	10
B) Bioconversions	15
B1) General Reaction Conditions	15
B2) Individual Reactions	16
V. Bioconversion in Methanol	21
VI. Initial Rate Studies	22
A) Axial Mutants (H136A, D134A, T187A) MtaC Screening	22
B) Initial Rate Measurements	23
VII. GCMS Calibration Curves	23
VIII. Synthetic Procedures	30
IX. Mass Spectra	43
X. References	48

I. Supplementary Figures

Figure S1. 15% SDS-PAGE of purified DhaF4611, (21 kDa), MtaC (24 kDa), and TCP (26 kDa). A single band was observed for all proteins without any impurity. ICPMS analysis (following the procedure from protein preparation section C) revealed 98%, 84%, 87% and 94% reconstitution of hydroxocobalamin for DhaF4611, MtaC, TCP and CarH* respectively.

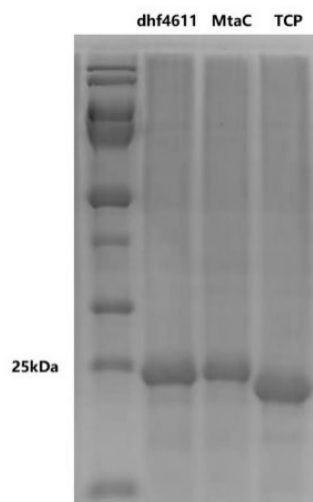


Figure S2. Comparison for *p*-methoxystyrene alkylation using CarH* and MtaC and T187A (MtaC).

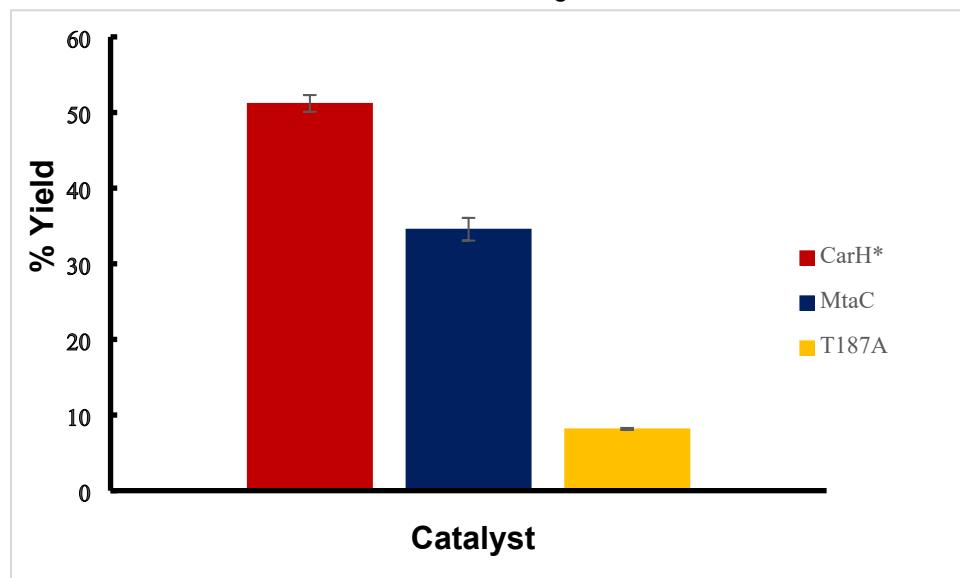
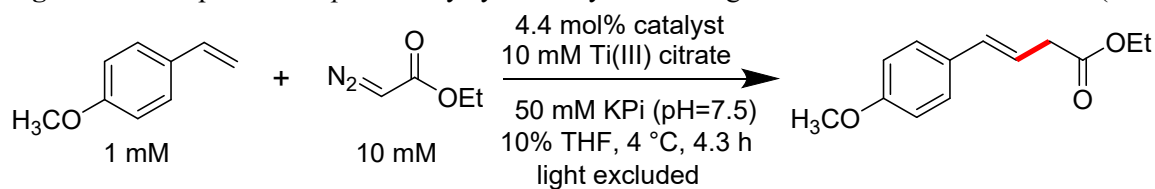


Figure S3. CD spectra of different corrinoid proteins representing their secondary structure in pure MeOH and MtaC in 6 M guanidinium hydrochloride solution.

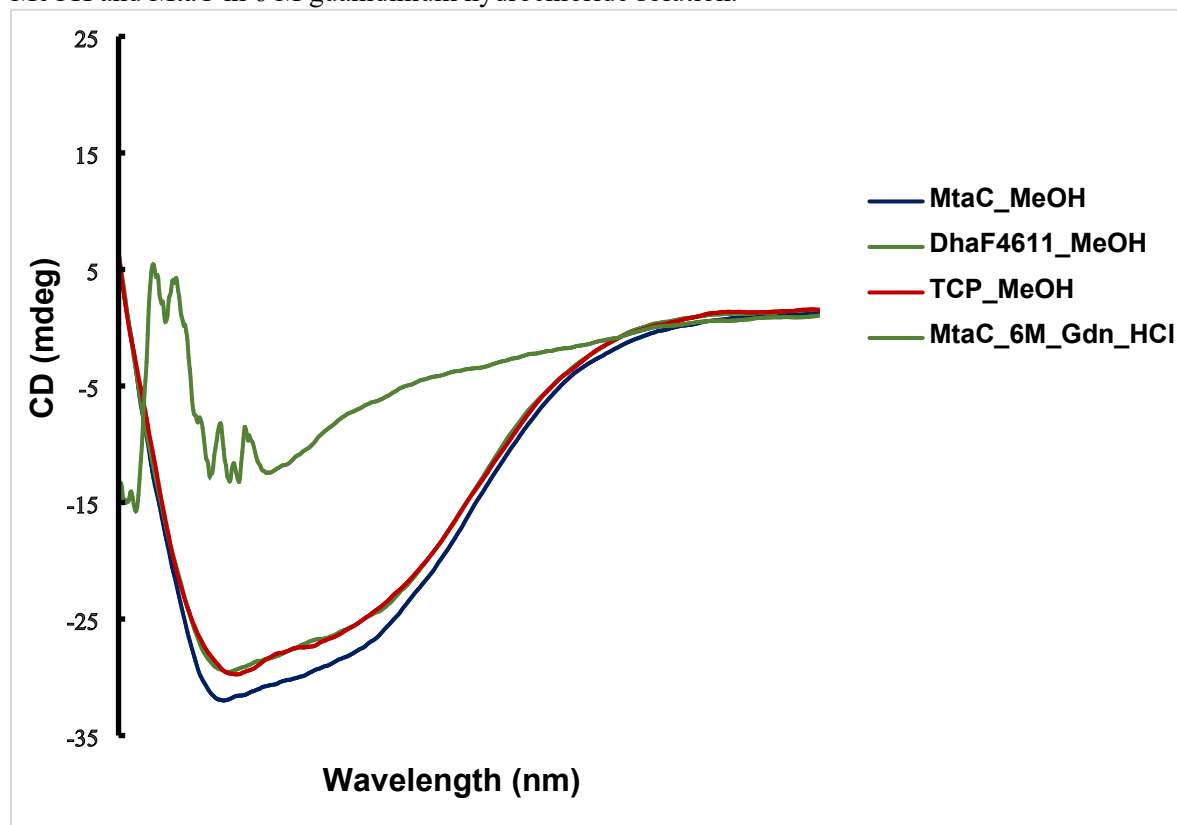
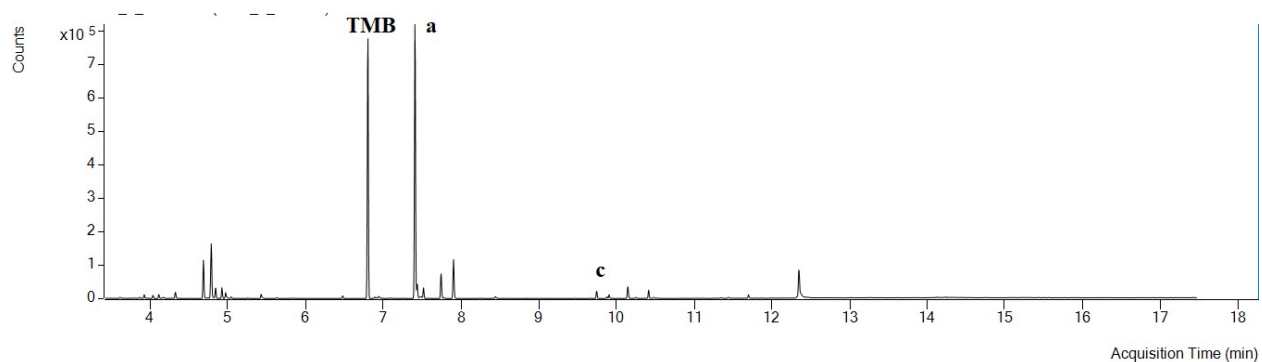
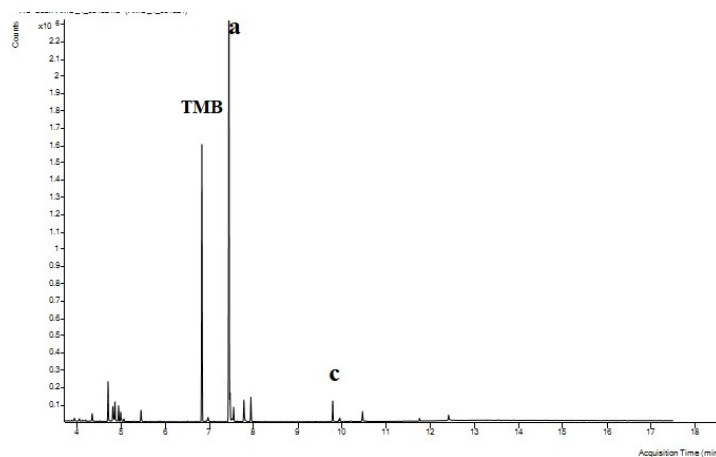


Figure S4. Time course for alkylation reaction showing formation of dialkylated product at long times.

A. GC trace obtained after 4h of bioconversion, peak c in the chromatogram corresponds to dialkylated product (area of c/ area of 1,3,5-trimethoxybenzene (TMB) 0.065):



B. GC trace acquired after 8 h of bioconversion. Ratio of area of c over TMB was 0.11:



C. GC trace obtained after 12 h of bioconversion. Ratio of area of c over TMB was 0.85:

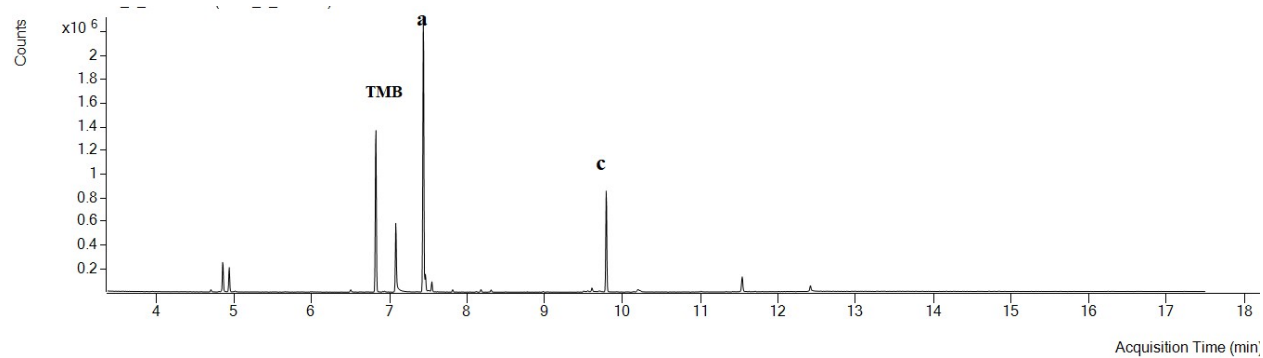


Figure S5. Graph showing conversions (following scheme 1) for second sphere variants

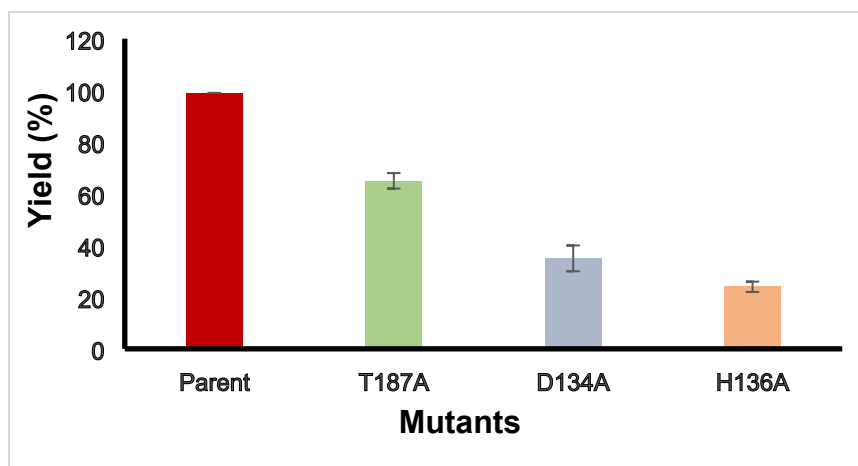
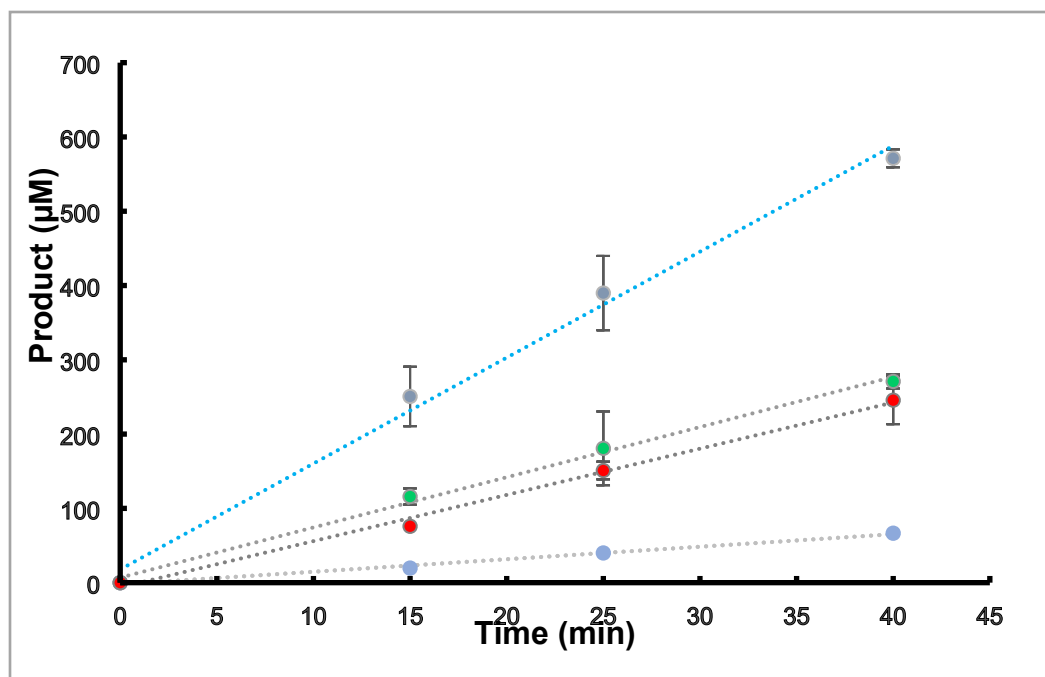


Figure S6. Graph showing initial rates of second sphere variants.



II. Materials and Instruments

A) Materials

Analytical scale bioconversions were carried out in a 2 mL vial with a screw cap purchased from Agilent Technologies. Ti(III) chloride 20% (w/w) in 3% hydrochloric acid was purchased from VWR Scientific (Radnor, PA). Ti(III) citrate was prepared by mixing 3.75mL of Titanium(III) chloride 20% (w/w) solution with 50mL of 200 mM sodium citrate solutions⁴. The pH of final solutions was adjusted to 7.5 using sodium carbonate. The concentration of Ti(III) citrate was determined by absorbance at 547nm ($\epsilon=100\text{M}^{-1}\text{cm}^{-1}$). All aniline substrates (except **1n**) were ordered from Sigma Aldrich (St.Louis, MO) or Combi-Blocks (San Diego, CA). Substrate **1n** was prepared by following the previously described procedure⁶. Standards for compounds **1a-g** were available commercially from Combi-Blocks. 1,3,5-Trimethoxybenzene internal standard was purchased from Sigma Aldrich. Luria broth (LB) was bought from Research Products International (Mt. Prospect, IL). Miniprep Kits and Ni-NTA superflow cartridges were purchased from QIAGEN, Inc (Valencia, CA) and used according to the manufacturer's instructions. Ni-NTA resin was purchased from Fisher Scientific (Hampton, NH). PageRuler™ Plus Prestained Protein Ladder, 10 to 250 kDa (Catalog number: 26619) was purchased from Fischer Scientific (Ipswich, MA). Primers used for cloning were purchased from Sigma Aldrich (St. Louis, MO). PrimeSTAR HS DNA Polymerase was purchased from Takara Bio (Mountain View, CA). Restriction enzymes, CutSmart® buffer, ligation enzymes, and ligation buffer were purchased from New England Biolabs (Ipswich, MA). The plasmids harboring the synthesized genes were purchased from Twist Bioscience (South San Francisco, CA).

B) Instruments

GC-MS analysis for bioconversions was performed by using Agilent 6890N Network Gas Chromatograph equipped with a module 7683B series autosampler and an Agilent 5975 mass selective detector. Analytical-scale bioconversions were analyzed by GC-MS using a 30m DB5 column (0.25 mm id 0.25 mm DF) from Agilent Technologies (Santa Clara, CA). ¹H NMR spectra were recorded at room temperature on Varian

I400, Varian I500, or Bruker B500 spectrometers. Chemical shifts are reported in ppm from tetramethylsilane with the solvent resonance as the internal standard. Data are reported as follows: chemical shift, multiplicity (s = singlet, d = doublet, t = triplet, q = quartet, br = broad, m = multiplet), coupling constants (Hz), and integration. ¹³C NMR spectra were obtained from the Bruker B500 instruments with complete proton decoupling. Chemical shifts are reported in ppm from tetramethylsilane with the solvent resonance as the internal standard (CDCl₃; δ77.16 ppm).

C) Software

NMR spectra were processed using MestReNova 11.0. GC-MS data were analyzed by MassHunter Software B.09.00 from Agilent Technologies.

III. Enzyme Preparation

A) CarH Homologue Identification

The crystal structure of CarH (PDB ID 5C8F chain A) was used to query the DALI Protein Structure Comparison Server (<http://ekhidna2.biocenter.helsinki.fi/dali/>). The first ten entries from the server output, including the structures of MtaC, MMCP, and MetH are shown below.

```
<html><head></head><body><pre style="word-wrap: break-word; white-space: pre-wrap;"># Job: CarH
# Query: 5c8fA
# No: Chain Z rmsd lali nres %id PDB Description
1: 5c8d-E 28.4 7.8 267 280 100 MOLECULE: LIGHT-DEPENDENT
TRANSCRIPTIONAL REGULATOR CARH;
2: 2i2x-B 15.6 11.3 142 258 15 MOLECULE: METHYLTRANSFERASE 1;
3: 3ezx-A 15.6 4.2 190 212 18 MOLECULE: MONOMETHYLAMINE CORRINOID
PROTEIN 1;
4: 1k7y-A 13.9 6.0 133 577 14 MOLECULE: METHIONINE SYNTHASE;
5: 4hh0-A 13.1 6.3 185 383 20 MOLECULE: APPA PROTEIN;
6: 3hh0-A 11.2 12.8 89 134 22 MOLECULE: TRANSCRIPTIONAL
REGULATOR, MERR FAMILY;
7: 2zhg-A 10.8 12.6 83 121 17 MOLECULE: REDOX-SENSITIVE
TRANSCRIPTIONAL ACTIVATOR SOXR;
8: 6jni-A 10.5 11.7 84 145 23 MOLECULE: CADR;
9: 3ucs-B 10.4 6.4 90 100 18 MOLECULE: CHAPERONE-MODULATOR
PROTEIN CBPM;
10: 4r24-B 10.0 2.6 76 85 33 MOLECULE: HTH-TYPE TRANSCRIPTIONAL
REGULATOR TNRA;
```

B) Enzyme gene preparation

MtaC/DhaF4611/TCP/MMCP design.

The DhaF4611 from *Methanosarcina barkeri* was obtained from the paper Grimm, 2020.¹ The MtaC from *Methanosarcina barkeri* was obtained from The Universal Protein Resource (Uniprot ID: Q46EH4). The TCP from *Methanosarcina barkeri* was obtained from The Universal Protein Resource (Uniprot ID: O93659). The sequence of His₆ was added to the N-terminus of the native MtaC sequence. The MtaC sequence and TCP sequence were found by blast search against the MethH COB domain sequence and CarH

sequence. The sequence was optimized, synthesized, and subcloned into pET28a⁺ by *Twist Bioscience* for *E.Coli* expression. The entire DNA sequences of each protein are shown below:

MtaC (Uniprot ID: Q46EH4)

ATGGGTCATCATCACCATCACCACCACGGTTCTAGCGGGAGCTCGATGCTTGATTTACCCGAGGCCTCGC
 TGAAAAAGGTACTCACGCGTTACAACGTAGCATTAGAAAAAGCGCTTACGCCAGAGGAAGCAGCTGAAGA
 ACTCTACCCCAAGGATGAGCTGATCTACCCCATTGCGAAAGCCATTTTTGAAGGAGAAGAAGATGATGTT
 GTCGAGGGACTTCAAGCTGCAATTGAGGCGGGGAAAGACCCGATCGATTTAATTGATGATGCGCTGATGG
 TTGGTATGGGGGTGGTATCCGTCTGTATGATGAAGGAGTAATTTTTCTGCCTAATGTCATGATGTCCGC
 GGATGCAATGTTGGAAGGCATTGAATACTGCAAAGAAAACAGTGGTGCGACCCCTAAAACAAAAGGTACA
 GTCGTTTGCCATGTGGCCGAAGGGGATGTACATGACATCGGGAAAAACATTGTGACCGCCCTCTTACGCG
 CGAACGGGTATAATGTGGTGGACCTGGGACGTGATGTGCCAGCGGAAGAGGTGCTGGCAGCAGTGCAGAA
 AGAGAAACCGATCATGCTCACGGGTACCGCACTTATGACGACGACGATGTATGCCTTCAAAGAAGTTAAT
 GATATGCTGTTGGAGAACGGGATTAAGATTCCGTTTGGCTTGGCGGGCGGCGCGGTGAACCAGGACTTCG
 TGAGCCAGTTCGCATTGGGCGTCTACGGTGAAGAAGCCGCAGATGCCCAAAAATCGCGGATGCGATTAT
 TGCAGGTACAACCGATGTTACGGAGTTACGGGAAAAATTTCATAAACAT**TAA**.

MtaC mutagenesis

Point mutations H136A, D134A, and T187A were introduced using overlap extension (SOE) PCR methods^{3,4}. The first step involved in the fragmentation PCR of the MtaC insert between NcoI and XhoI restriction sites using 1) a forward mutagenic primers with an insert-specific non-mutagenic reverse primers, and 2) reverse mutagenic primers with an insert-specific non-mutagenic forward primer. The fragmentation PCR products were treated with 1 unit DpnI in 30 µL of 1X NEB cutsmart buffer and purified by Qiagen PCR products purification kit. The assembly reactions were conducted using insert-specific non-mutagenic primers and the respective fragmentation PCR products. The assembled PCR products were purified by a 1% agarose gel and isolated using Qiagen gel purification kits. 1µg of the PCR products were digested by 1 unit of NcoI and 1 unit of XhoI enzymes in 50 µL of 1X NEB cutsmart buffer at 37 °C for 4 h, while 1µg of template plasmids were digested by the same conditions for 1h. The digested products were purified over 1% agarose gel and isolated using Qiagen gel purification kits. Ligations of the insert sequences into pET 28a⁺ were carried out by using 1 unit of T4 ligase with 1:10 molar ratio of digested PCR products and the double-digested pET28a (NcoI and XhoI) in 20 µL of 1X T4 ligation buffer at 22 °C for 3 h. The plasmids were purified by Qiagen PCR purification kits for transformations. Plasmid DNA was extracted from BL21 cells after transformation, and sequenced by Quintarabio (Cambridge, MA) to confirm the results.

Table S1. Primer design for SOE-PCR

Primer Name	Sequence
Insert specific non-mutagenic F.P.	GGAGATATACCATGGGTCATCATCACC
Insert specific non-mutagenic R.P.	GGTGGTGTCTCGAGTTAATGTTTATGAAA
H136A F.P.	AAGGGGATGTAGCCGACATCGGGAAAAACA
H136A R.P.	TGTTTTTCCCGATGTCGGCTACATCCCCTT
D134A F.P.	CATGTGGCCGAAGGGGCTGTACATGACATC
D134A R.P.	GATGTCATGTACAGCCCCTTCGGCCACATG
T187A F.P.	ATGACGACGGCCATGTATGCCTTCAAAGAA
T187A R.P.	TTCTTTGAAGGCATACATGGCCGTCGTCAT

DhaF4611 (Uniprot ID: B8FXL1)

ATGGGAAGTTCCCACCATCATCACCATCACCATTCAAGCGGCATGAGCAAAATTGCGGAGGTCAAGGCTA
TGGTGAAGCTGGGAAGGCCAAACTCGTGCCTGGTCTGGTTTCAGGAAGCATTAGACGCCGGTAACGCAGC
AGGCGATATTCTGGCCGGGATGATCGATAGTATGGGCGTTGTGGGCGATAAGTTTAGCGCTGGTGAACGTG
TTTGTCCCGGAGATGCTGATGGCGGCCAAAGCGATGTCCAAAGGTGTGGATGTGCTGAAACCGCATCTTA
CAGGTGAGAGCGCTACGAGCCTGGGTACTTGTGTAATTGGTACAGTAGCGGGGGACCTGCACGATATTGG
CAAAAATCTGGTAGCAATGATGCTGGAATCGGTTGGTTTTCAATGTGGTGGATCTGGGCGTGGATGTGTGC
GCCGAGAAATTCGTTGACGCCGTTCTGTAATAATGACAATGTGAAGATTGTGGCTTGTAGCGGCCCTCTTGA
CGACGACCATGCCTGCAATGAAAGAAACCGTTCAATCACTGAAAACTCGGGACTGACTGGGTTTAAAGT
GATTGTCCGTGGTGCGCCGTGTCTCAAGCCATGGCCGACGAAATCGGGGCCGATGGGTTTGCTCCAGAT
GCAGGGGGGGCAGCCGTCAAGGCCAAAGAACTGGCCCATGCAGTTGACT**TGA**

TCP (Uniprot ID: O93659)

ATGGGTCACCACCATCATCACCACCATGGCTCGTCTGGCTCTTCGATGGCAAACCAGGAGATCTTTGATA
AGCTGCGTGATGCTATCGTCAACCAAAACGTTGCAGGTACCCAGAGCTGTGCAAAGAAGCCCTGGCGGC
AGGCGTACCGGCCCTTAGATATTATTACCAAAGGTCTGTCTGTAGGCATGAAAATCGTGGGCGATAAATTC
GAGGCCGAGAAATCTTTCTGCCGAGATCATGATGTCTGGTAAGGCCATGTCTAACCGCATGGAAGTTC
TGACACCCGAATTAGAGAAGAATAAGAAAGAGGGTGAAGAAGCCGGTCTGGCCATTACCTTTGTGGCGGA
AGGTGACATCCATGATATCGGCCATCGCCTGGTACTACCATGCTGGGCGCAAATGGATTTCAAATCGTC
GATCTGGGGTTGATGTGCTGAACGAAAACGTTGTGGAAGAAGCGCCAAACATAAAGGTGAAAAAGTAC
TTCTGGTCCGTAGTGCCTGATGACCACCAGCATGCTGGGTCAGAAAGACCTGATGGATCGCCTGAATGA
AGAGAACTCCGCGACTCGGTGAAATGCATGTTTGGCGGCGCGCCTGTGTCTGATAAATGGATTGAAGAA
ATTGGCGCTGACGCAACGGCAGAAAATGCGGCCGAGGCCGCGAAGGTGGCGCTTGAAGTGATGAAAT**TGA**

MMCP (Uniprot ID: O30641)

ATGGGTCACCACCATCATCACCACCATGGCTCGTCTGGCTCTTCGATGGCAAACCAGGAGATCTTTG
ATAAGCTGCGTGATGCTATCGTCAACCAAAACGTTGCAGGTACCCAGAGCTGTGCAAAGAAGCCCT
GGCGGCAGGCGTACCGGCCCTTAGATATTATTACCAAAGGTCTGTCTGTAGGCATGAAAATCGTGGGC
GATAAATTCGAGGCCGAGAAATCTTTCTGCCGAGATCATGATGTCTGGTAAGGCCATGTCTAACG
CGATGGAAGTTCTGACACCCGAATTAGAGAAGAATAAGAAAGAGGGTGAAGAAGCCGGTCTGGCCAT
TACCTTTGTGGCGGAAGGTGACATCCATGATATCGGCCATCGCCTGGTACTACCATGCTGGGCGCA
AATGGATTTCAAATCGTGCATCTGGGGTTGATGTGCTGAACGAAAACGTTGTGGAAGAAGCGGCCA
AACATAAAGGTGAAAAAGTACTTCTGGTCCGTAGTGCCTGATGACCACCAGCATGCTGGGTCAGAA
AGACCTGATGGATCGCCTGAATGAAGAGAACTCCGCGACTCGGTGAAATGCATGTTTGGCGGCGCG
CCTGTGTCTGATAAATGGATTGAAGAAATGGCGCTGACGCAACGGCAGAAAATGCGGCCGAGGCCG
CGAAGGTGGCGCTTGAAGTGATGAAAT**TGA**

Transformation

Electro-competent BL21(DE3) *E. coli* cells were transformed by pET28a+ plasmids containing each enzyme insert between NcoI and XhoI restriction sites via electroporation and immediately recovered in 750 µL SOC medium. The cultures were incubated at 37 °C for 45 min. Then, the cells were spread on an LB agar plate containing 50 µg/mL kanamycin and incubated at 37 °C for 16 h. A single colony was used to inoculate 5mL LB media containing 50 µg/mL kanamycin, and the cells were cultured at 37 °C for 16 h. 1 mL of this culture was combined with 1 mL of 50% glycerol, and the resulting cell suspension was stored at -80 °C until further use. The recombinant plasmid containing the DNA template was extracted from overnight culture by QIAprep® miniprep kit with using protocols provided by the manufacturer and sequenced by Quintarbio.

C) Protein Preparation

7 mL overnight cultures were used to inoculate 1 L LB media containing 50 µg/mL kanamycin. The cultures were incubated at 37 °C until $OD_{600}=0.6$. Gene expression was induced by 1 mL of 1 mM IPTG at 16 °C for 18 h, and cells were harvested by centrifugation (3,200 g for 10 min). After the supernatant was discarded, the cells were resuspended into 10 mM imidazole buffer containing 50 mM sodium phosphate and 300 mM sodium chloride (pH=7.5) and stored at -80 °C until lysis. The cells were lysed by sonication at 4 °C for 5 min (30 s on/45 s off; 40 W). The crude extract was obtained after centrifugation at 31,000 x g and 4 °C for 20 min. The crude extract was mixed by end-over-end rotation with 5 mL Ni-NTA resin for 40 min and loaded into a gravity column. The repacked column was washed by 100 mL column wash buffer (20 mM imidazole, 50 mM sodium phosphate, and 300 mM sodium chloride, pH=7.5) to remove nonspecifically bound protein. The POI containing a His₆ tag was eluted by using 60mL elution buffer containing 300 mM imidazole, 50 mM sodium phosphate and 300 mM sodium chloride (pH=7.5). The purified protein was dialyzed by 2X4L KPi buffer at pH=7.5 for overnight.

The protein purity was evaluated by 15% SDS-PAGE as shown above in Figure S1, and similar SDS-PAGE analysis of the crude lysate and cell pellet is provided below in Figure S5 showing that very little enzyme is left in the pellet after lysis.

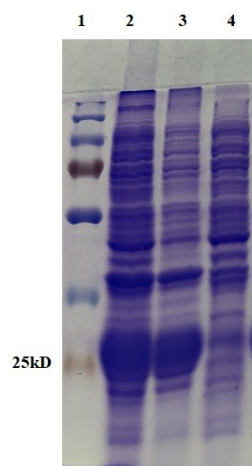


Figure S7. Attached above is the 15% SDS-PAGE. Lane 1 corresponds to the molecular weight marker, lane 2 corresponds to the lysate showing MtaC band around 25kD. Lane 3 is the 1:1 dilution of lysate in buffer. Lane 4 is the cell debris obtained after clarification.

B12 Reconstitution

The holo-enzyme was obtained by incubation of apo-MtaC with hydroxocobalamin in a 1:3 ratio⁷. Excess B12 was removed by SEC column purification on an FPLC. The FPLC is a GE AKTA purifier equipped with a UPC-900 detector (monitoring absorbance at 280 nm) and P-900 pumps using a size-exclusion column (SEC). A HiLoad 16/600 Superdex 200 column (GE Life Sciences) was equilibrated 2 CVs of the mobile phase (50 mM Na₃PO₄, 150 mM NaCl at pH=7.5). The flow rate was set to 1 mL/min and fractions were manually collected (the proteins of interest eluted between 50-95 mL). Samples were then concentrated and diafiltration was performed with 15 kDa Amicon ultra centrifugal filters at 3200g for 2 h. The amount of B12 incorporated was determined by both ICP-MS and UV-Vis (@ 525 nm).

The initial rates from Figure S4 were divided by the ICP-MS reconstitution yields to obtain adjusted initial rates of 15.8, 8.2, 11.9, and 2.4 $\mu\text{M}/\text{min}/([\text{MtaC}_{\text{holo}}]/[\text{MtaC}_{\text{apo}}])$ for parent MtaC, T187A, D134A, and H136A respectively.

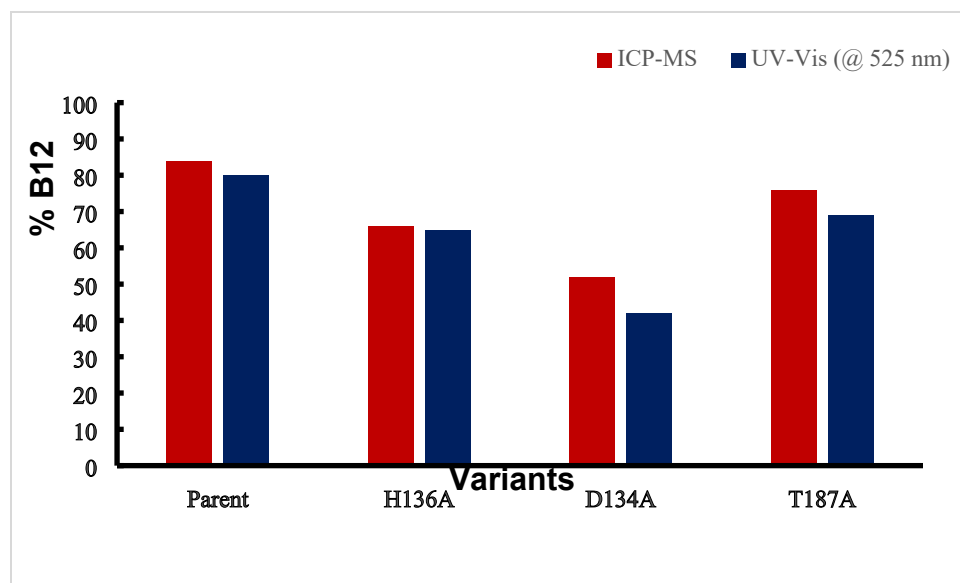


Figure S8. Plot depicting the B12 reconstitution efficiency by parent MtaC and axial variants of MtaC H136A, D134A, and T187A using ICP-MS technique as well as UV-Vis measurement at 525 nm.

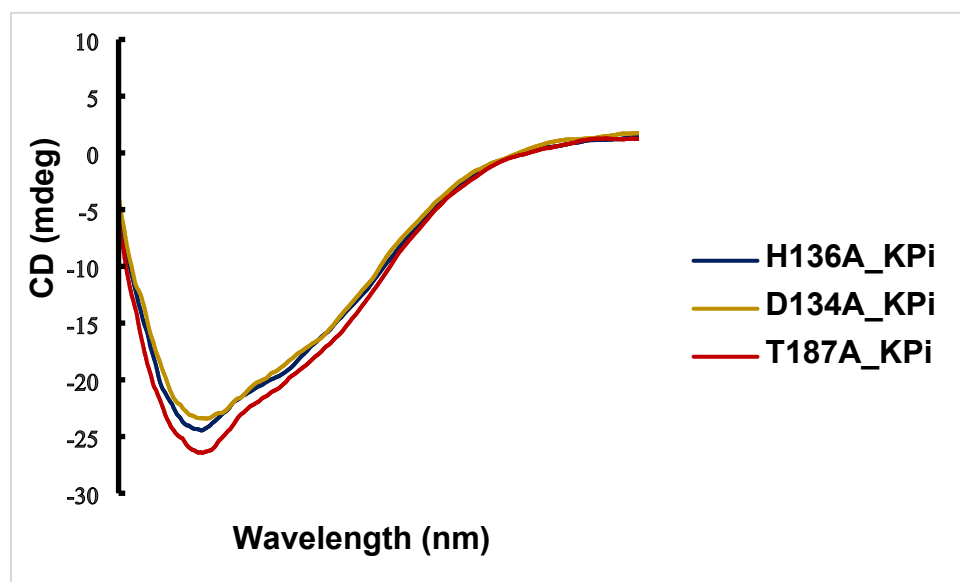


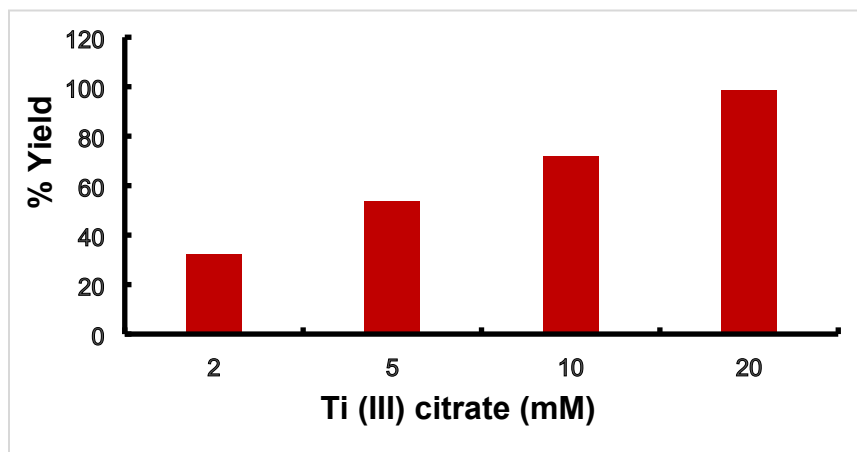
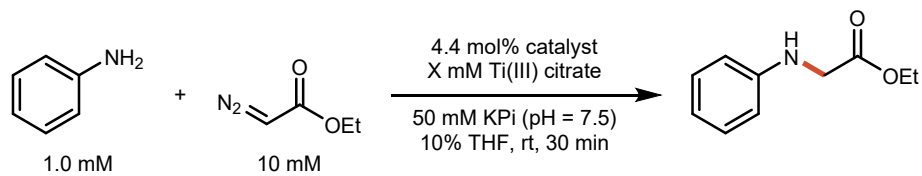
Figure S9. CD spectra of alanine variants of H136, D134 and T187 residues in 50 mM KPi buffer.

IV. Bioconversion Protocol and Analysis

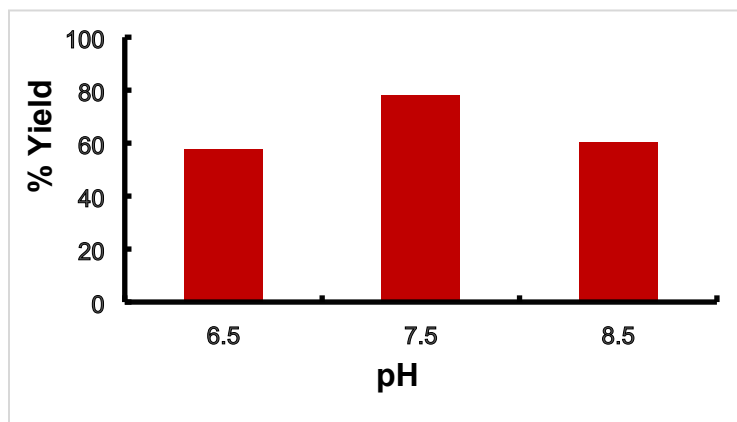
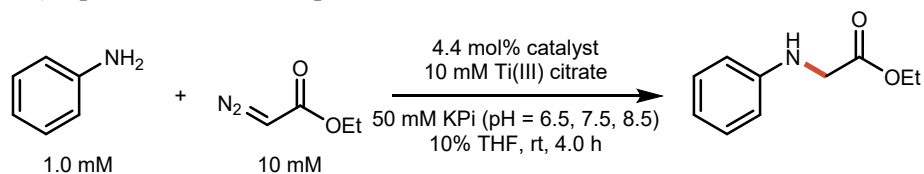
All data contained in the charts below is provided in the supplemental data file (MtaC_data_file.xlsx).

A) Reaction Optimization

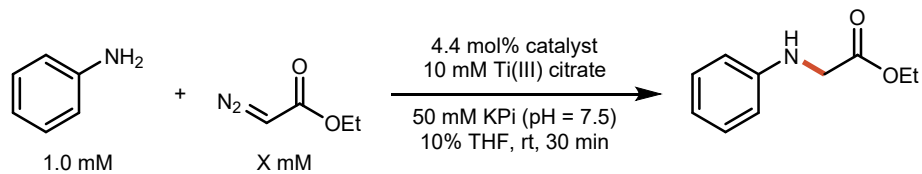
A1) Reducing agent concentration optimization.

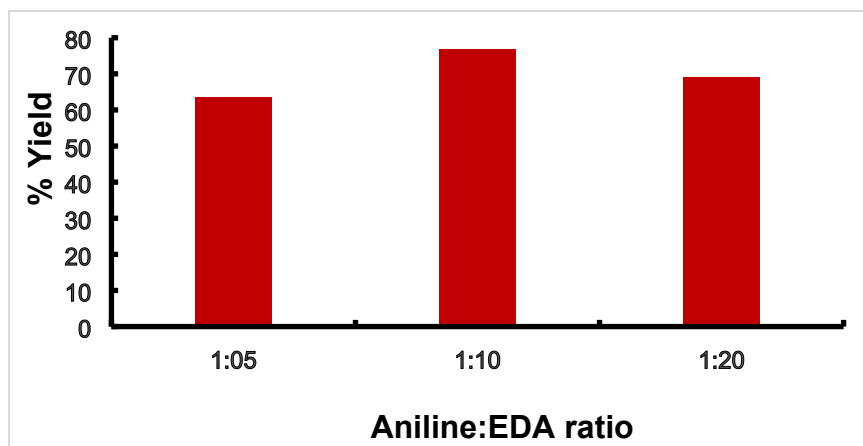


A2) Optimization with respect to buffer.

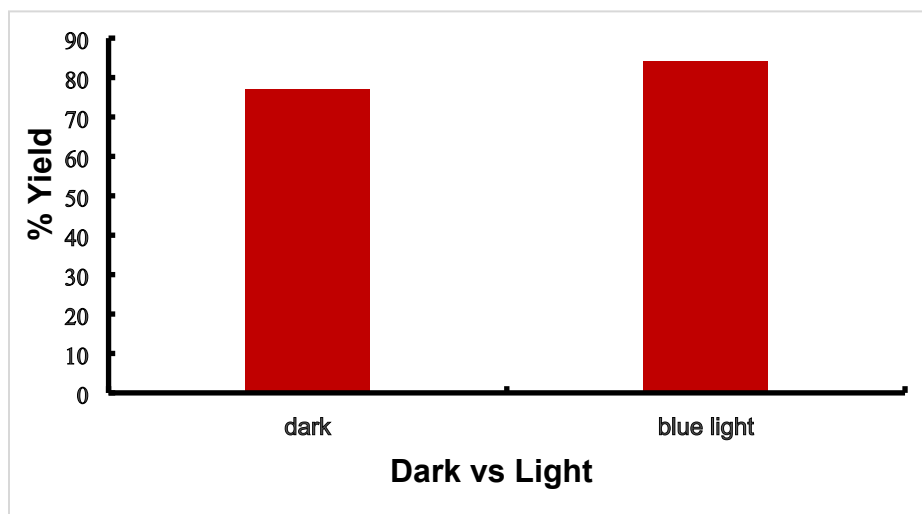
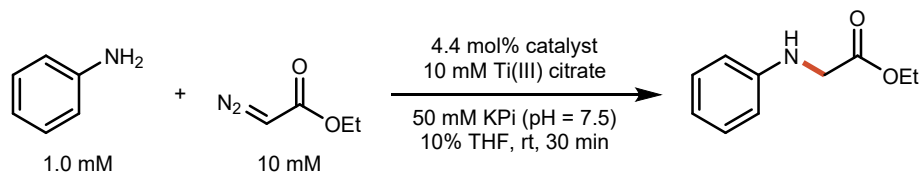


A3) Optimization with different ratio of Aniline to EDA.

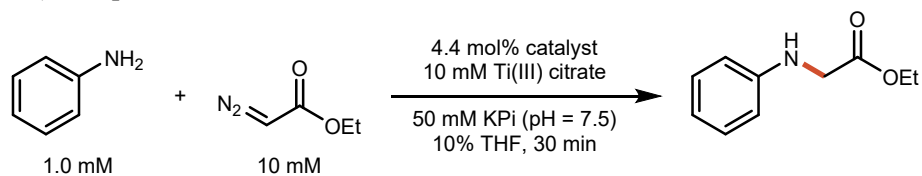


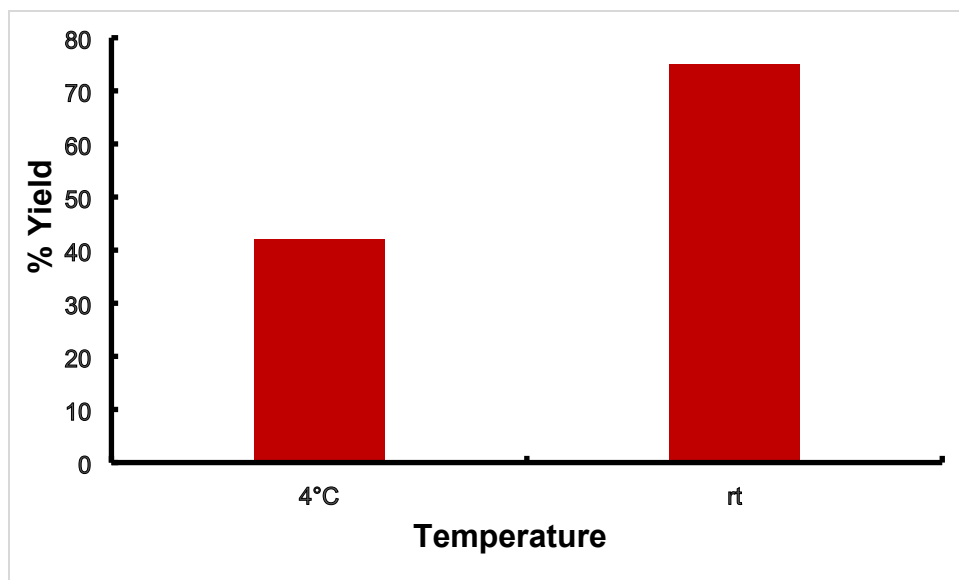


A4) Dark vs light condition.

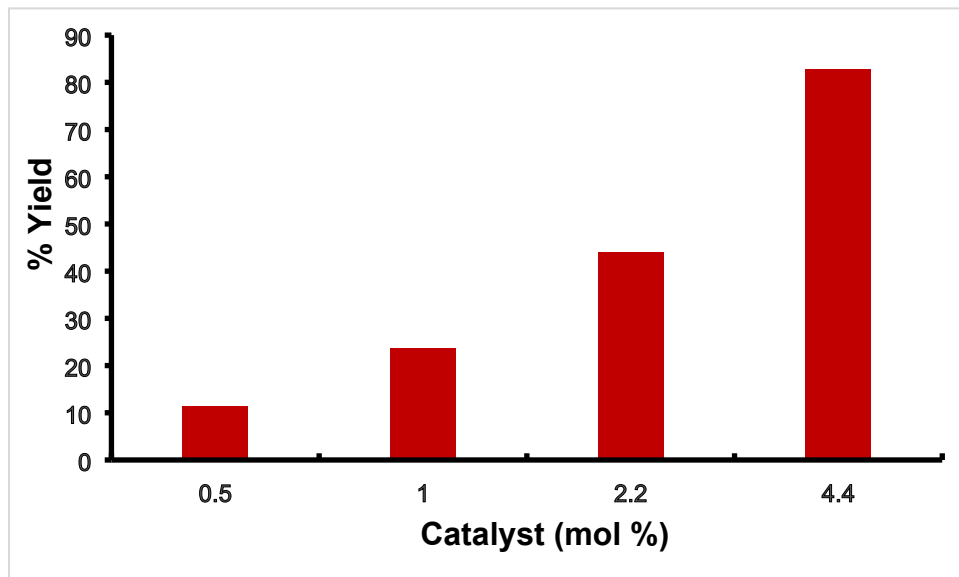
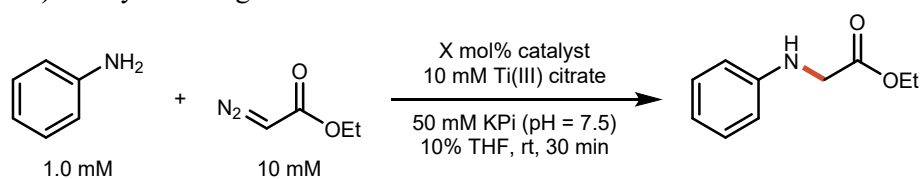


A5) Temperature effect.

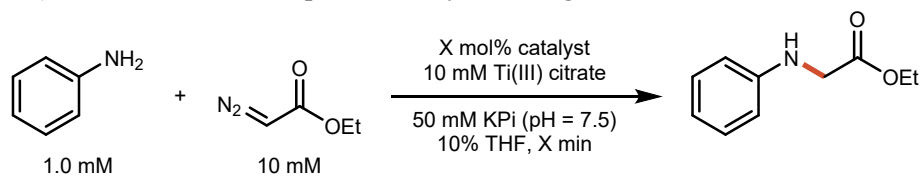


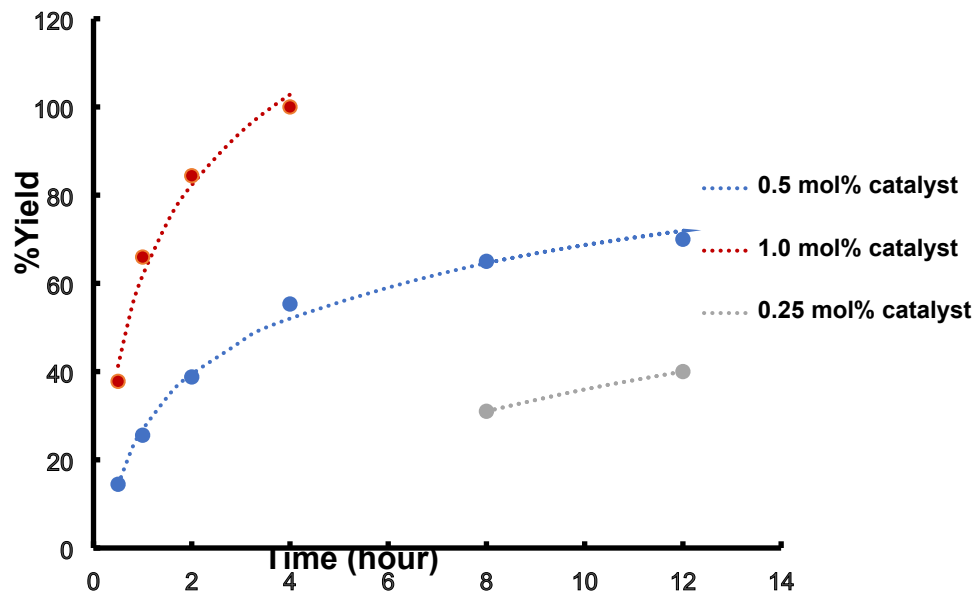


A6) Catalyst loading.

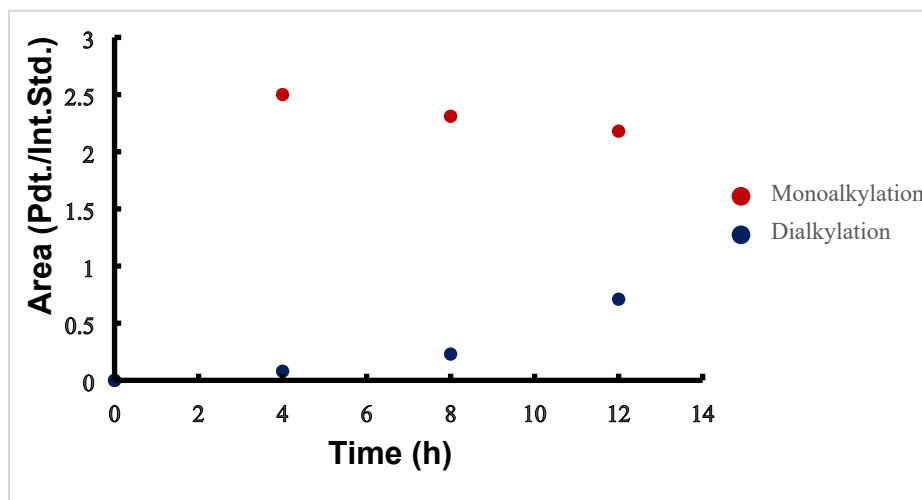
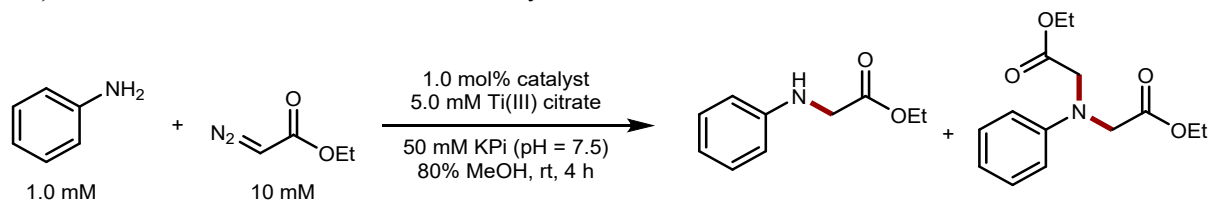


A7) Time course with respect to catalyst loading.



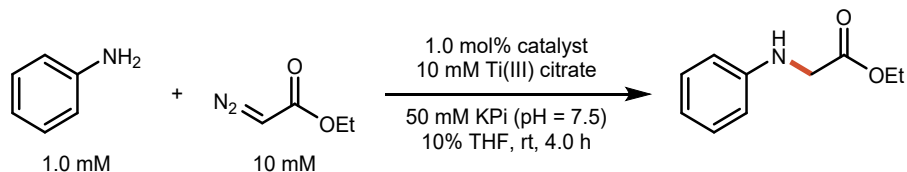


A8) Time course to monitor mono- vs di-alkylation in MeOH



B) Bioconversions

B1) General Reaction Conditions



Aniline alkylation bioconversions were set up in the wetbox under N₂ atmosphere using a 2 mL air free Agilent glass HPLC sample vial. Bioconversion reactions were set up by adding aniline and ethyl diazoacetate (EDA) in 50 mM KPi-THF into the reaction vial, followed by the addition of catalyst (preincubated with reducing agent for 1 min) at room temperature. Total reaction volume was 800 μ L for the analytical scale of bioconversions. The final concentration of each reagents were: 1 mM aniline, 10 mM EDA, 1 mol% catalyst, 10mM Ti(III) citrate, 10% THF. After the reaction setup, the reaction vials were agitated by end-over-end rotation for 4h at RT. After completion of the bioconversion, the reactions were quenched by the addition of 800 μ L of ethyl acetate containing 480 nmol of internal standard 1,3,5-Trimethoxybenzene (TMB). The reaction mixture was collected in 2 mL Eppendorf vial and further centrifuged to separate the organic layer. Organic components were analyzed by GC-MS. Yields were determined by GC-MS relative to internal standard using response factors derived from authentic standards (see section VII below). A summary of relevant peak integrations is provided in Table S2.

Table S2. Formation of monoalkylated vs dialkylated product for the substrates included in manuscript Scheme 1 from raw integration values in the GC chromatograms as ratios relative to trimethoxy benzene (TMB) internal standard.

Entry	Substrate	Substrate Remaining (S/TMB) ratio	Monoalkylation Product/ TMB ratio	Dialkylation Product/ TMB ratio
1	1a	0	3.40	0.07
2	1b	0	4.07	0.45
3	1c	0.32	5.13	0.06
4	1d	0.25	4.50	0.30
5	1e	0	3.85	0.14
6	1f	0.10	4.29	0.02
7	1g	0	7.10	0.01
8	1h	0.35	2.70	<0.01
9	1i	0.27	3.72	<0.01
10	1j	0.20	3.05	0.02
11	1k	0.30	2.75	0.01
12	1l	0.03	4.05	0.01
13	1m	0.01	3.85	<0.01
14	1n	0.23	4.50	<0.01
15	1a,2b	0 (1a)	5.75	<0.01

B2) Individual Reactions

Reaction of **1a** and EDA was carried out using the general procedure described above. GC analysis showed the product **3a** at 7.4 min and TMB at 6.8 min. There was no trace of remaining aniline in the reaction. MS (EI): m/z (%) = 179.1 (25), 106 (100), 77 (20).

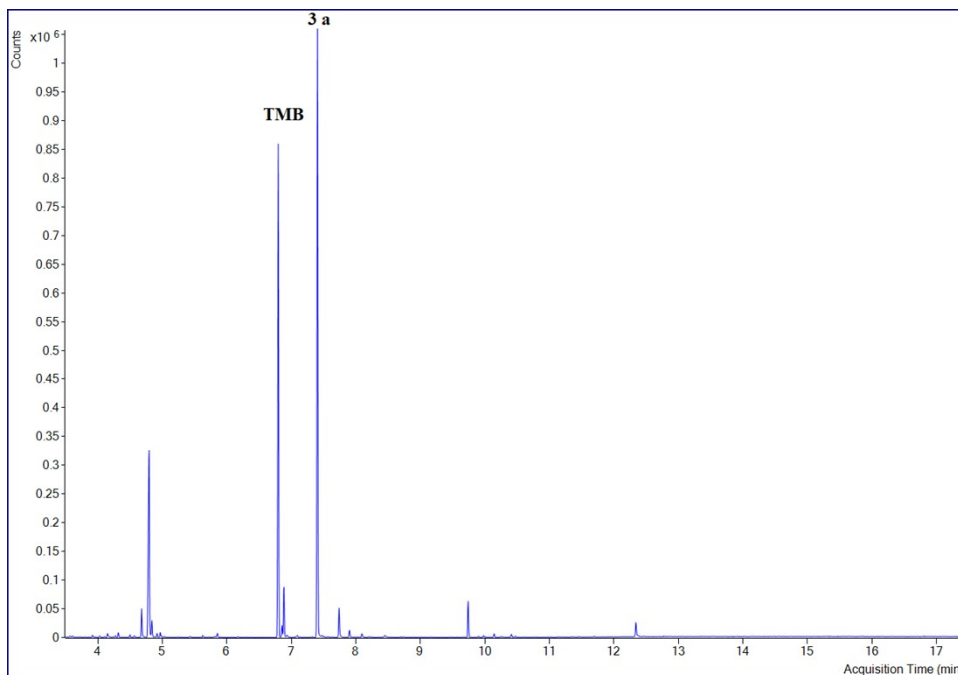


Figure S10. The above chromatogram represents the GC-trace of bioconversion using aniline and EDA as substrates. Product **3a** elutes at 7.4 min. Internal standard TMB elutes at 6.8 min.

Reaction of **1b** and EDA was carried out using the general procedure described above. GC analysis showed the product **3b** at 8.08 min and TMB at 6.8 min. There was no trace of remaining *para*-toluidine in the sample. MS (EI): m/z (%) = 193.1 (20), 120.1 (100), 91.1 (14).

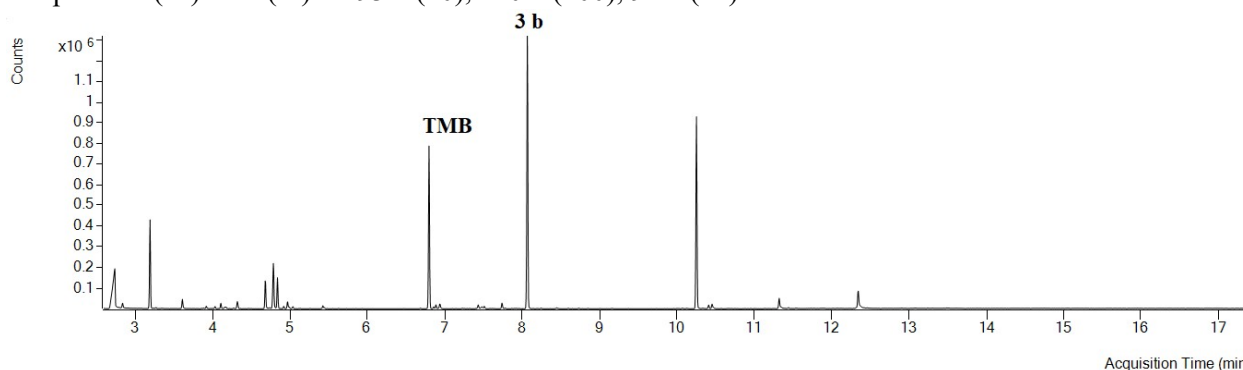


Figure S11. The above chromatogram represents the GC-trace of bioconversion using *para*-toluidine and EDA as substrates. Product **3b** elutes at 8.08 min. Internal standard TMB elutes at 6.8 min. Note, the peak near 10.3 min is the dialkylation product. While the area of this peak is significant, it is due to a large apparent response factor; the yield of **3b** relative to internal standard was twice validated as ~99%.

Reaction of **1c** and EDA was carried out using the general procedure described above. GC analysis showed the product **3c** at 7.91 min, and TMB at 6.8 min. There was no trace of remaining *ortho*-toluidine in the reaction. MS (EI): m/z (%) = 193.1 (30), 120.1 (100), 91.1 (20).

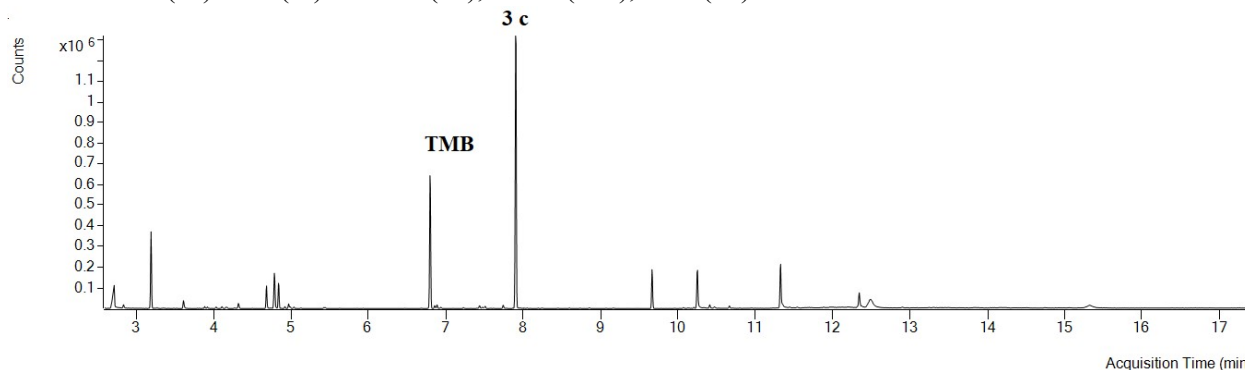


Figure S12. The above chromatogram represents the GC-trace of bioconversion using *ortho*-toluidine and EDA as substrates. Product **3c** elutes at 7.91 min. Internal standard TMB elutes at 6.8 min.

Reaction of **1d** and EDA was carried out using the general procedure described above. GC analysis showed the product **3d** retention at 8.05 min, and TMB at 6.8 min. There was no trace of remaining *meta*-toluidine in the reaction. MS (EI): m/z (%) = 193.1 (30), 120.1 (100), 91.1 (10).

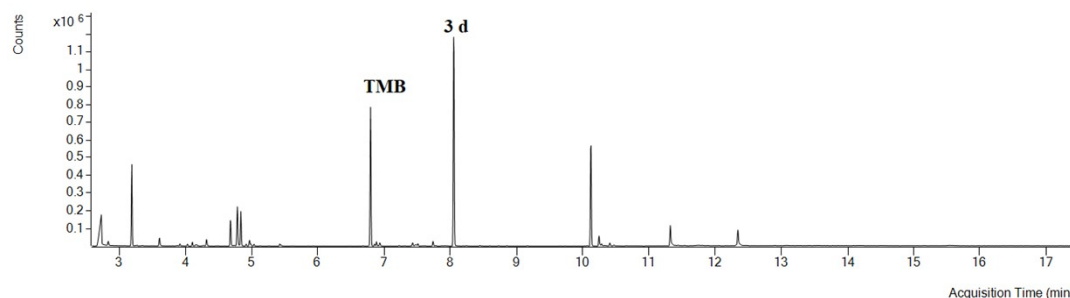


Figure S13. The above chromatogram represents the GC-trace of bioconversion using *meta*-toluidine and EDA as substrates. Product **3d** elutes at 8.05 min. Internal standard TMB elutes at 6.8 min. The peak near 10 min is again dialkylation product and, as noted in Figure S6, the large area of this peak is likely due to a large response factor for the dialkylated product.

Reaction of **1e** and EDA was carried out using the general procedure described above. GC analysis showed the product **3e** retention at 8.87 min, and TMB at 6.8 min. There was no trace of remaining *para*-chloroaniline in the reaction. MS (EI): m/z (%) = 213.1 (20), 140.1 (100).

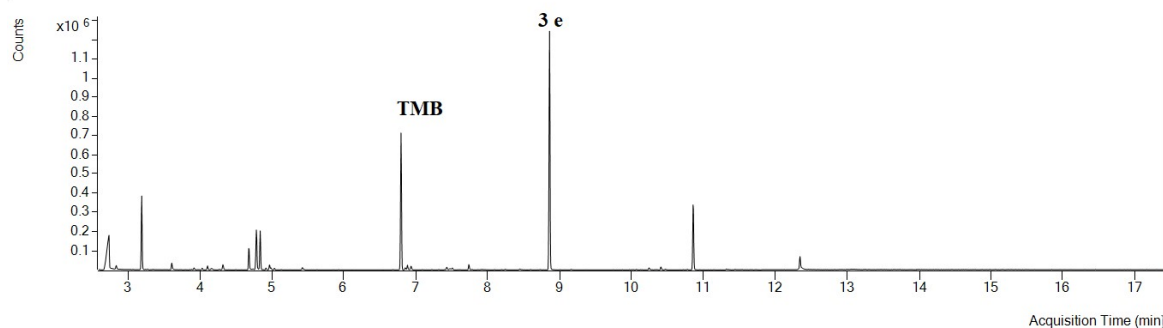


Figure S14. The above chromatogram represents the GC-trace of bioconversion using *para*-chloroaniline and EDA as substrates. Product **3e** elutes at 8.87 min. Internal standard TMB elutes at 6.8 min.

Reaction of **1f** and EDA was carried out using the general procedure described above. GC analysis showed the product **3f** retention at 8.78 min, and TMB at 6.8 min. There was no trace of remaining *meta*-chloroaniline in the reaction. MS (EI): m/z (%) = 213.1 (25), 140.1 (100).

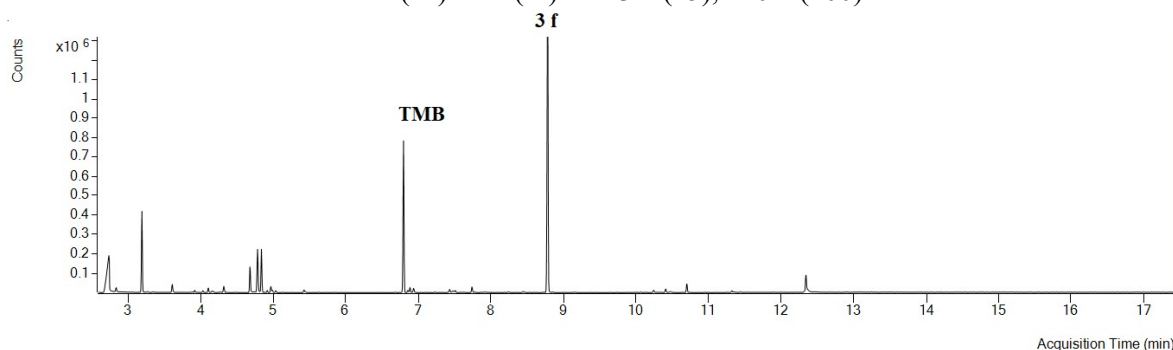


Figure S15. The above chromatogram represents the GC-trace of bioconversion using *meta*-chloroaniline and EDA as substrates. Product **3f** elutes at 8.78 min. Internal standard TMB elutes at 6.8 min

Reaction of **1g** and EDA was carried out using the general procedure described above. GC trace showed the product **3g** retention at 7.70 min, and TMB at 6.8 min. There was no trace of remaining *para*-trifluoromethyl aniline in the reaction. MS (EI): m/z (%) = 247.1 (15), 174.1 (100), 145.1 (13).

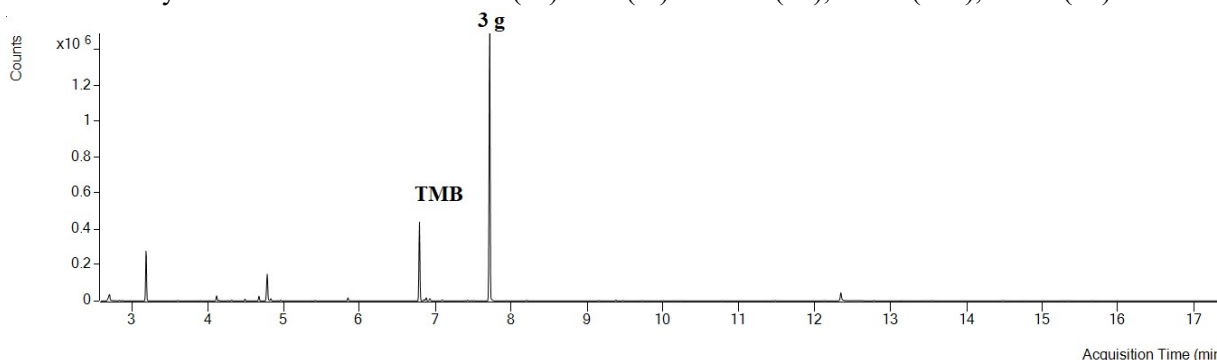


Figure S16. The above chromatogram represents the GC-trace of bioconversion using *para*-trifluoromethyl aniline and EDA as substrates. Product **3g** elutes at 7.70 min. Internal standard TMB elutes at 6.8 min.

Reaction of **1h** and EDA was carried out using the general procedure described above. GC trace showed the product **3h** retention at 10.56 min, and TMB at 6.8 min. The remaining *para*-aminoacetophenone was observed at 7.5 min. MS (EI): m/z (%) = 221.1 (25), 148.1 (100), 105.1 (10).

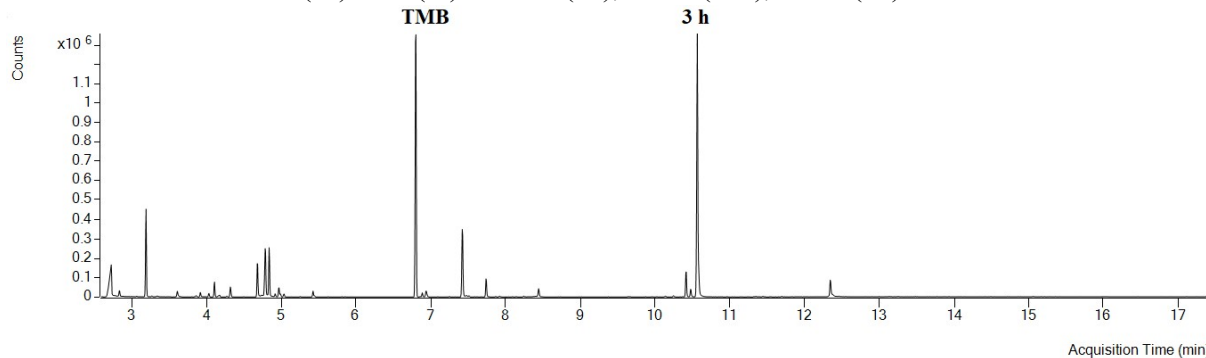


Figure S17. The above chromatogram represents the GC-trace of bioconversion using *para*-aminoacetophenone and EDA as substrates. Product **3h** elutes at 10.56 min. Internal standard TMB elutes at 6.8 min.

Reaction of **1i** and EDA was carried out using the general procedure described above. GC analysis showed the product **3i** retention at 10.99 min, and TMB at 6.8 min. The remaining benzocaine was observed at 8.0 min. MS (EI): m/z (%) = 251.1 (20), 178.1 (100), 150.1 (30), 105.1 (10).

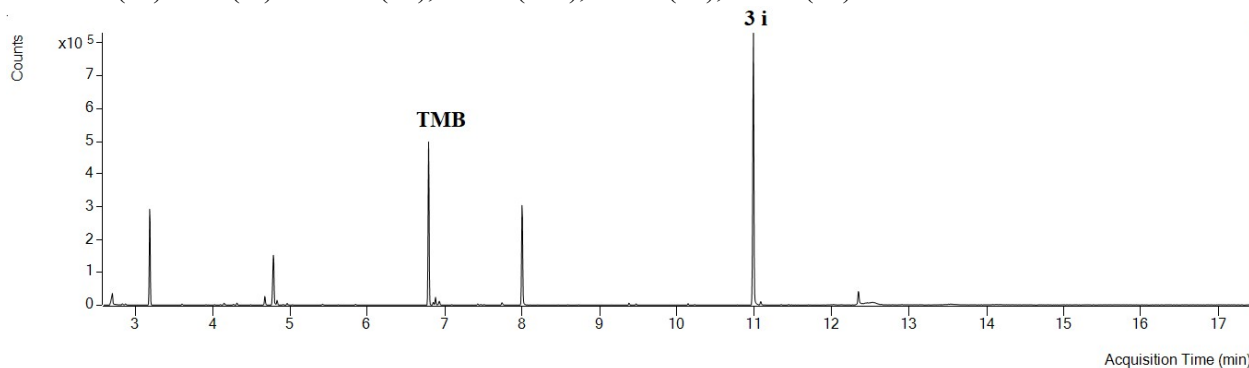


Figure S18. The above chromatogram represents the GC-trace of bioconversion using benzocaine and EDA as substrates. Product **3i** elutes at 10.99 min. Internal standard TMB elutes at 6.8 min.

Reaction of **1j** and EDA was carried out using the general procedure described above. GC analysis showed that product **3j** elutes at 9.01 min, and TMB at 6.8 min. There was no trace of remaining *para*-anisidine in the reaction. MS (EI): m/z (%) = 209.2 (20), 136.1 (100).

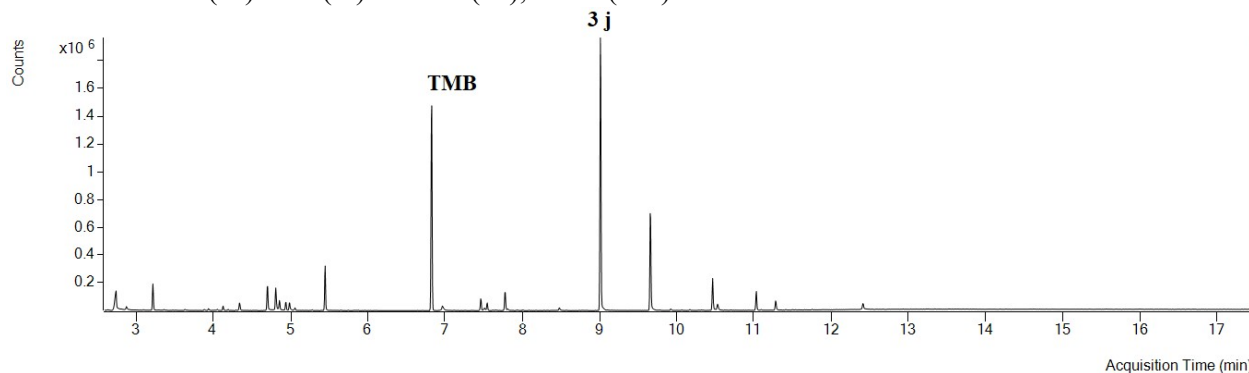


Figure S19. The above chromatogram represents the GC-trace of bioconversion using *para*-anisidine and EDA as substrates. Product **3j** elutes at 9.01 min. Internal standard TMB elutes at 6.8 min.

Reaction of **1k** and EDA was carried out using the general procedure described above. GC analysis showed the product **3k** retention at 9.1 min, and TMB at 6.8 min. There was no trace of remaining *meta*-anisidine in the reaction. MS (EI): m/z (%) = 209.2 (25), 136.1 (100).

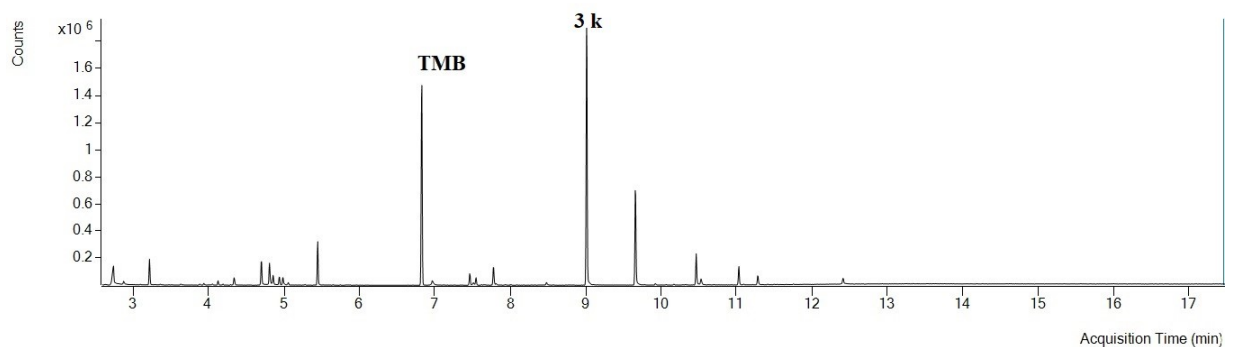


Figure S20. The above chromatogram represents the GC-trace of bioconversion using *meta*-anisidine and EDA as substrates. Product **3k** elutes at 9.1 min. Internal standard TMB elutes at 6.8 min.

Reaction of **11** and EDA was carried out using the general procedure described above. GC trace showed the product **31** retention at 8.43 min, and TMB at 6.8 min. There was no trace of remaining indoline in the reaction. MS (EI): m/z (%) = 205.1 (20), 132.1 (100), 117.1 (10).

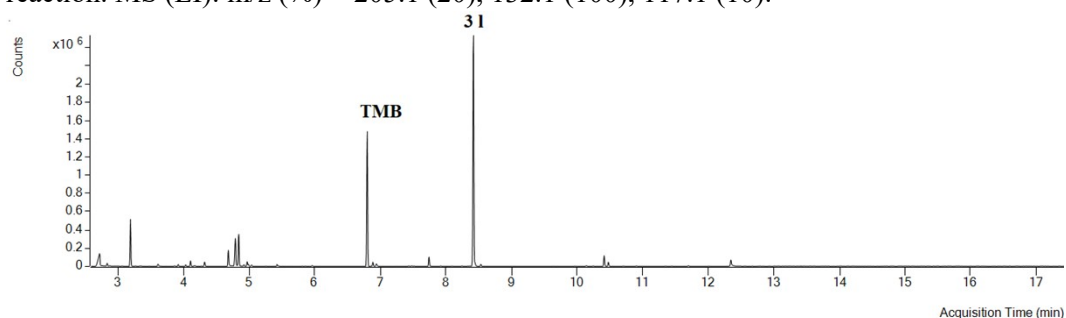


Figure S21. The above chromatogram represents the GC-trace of bioconversion using indoline and EDA as substrates. Product **31** elutes at 8.43 min. Internal standard TMB elutes at 6.8 min.

Reaction of **1m** and EDA was carried out using the general procedure described above. GC analysis showed the product **3m** retention at 9.16 min, and TMB at 6.8 min. There was no trace of remaining 1,2,3,4-tetrahydroquinoline in the reaction. MS (EI): m/z (%) = 219.2 (15), 146.1 (100), 130.1 (12), 118.1 (14), 91.1 (11).

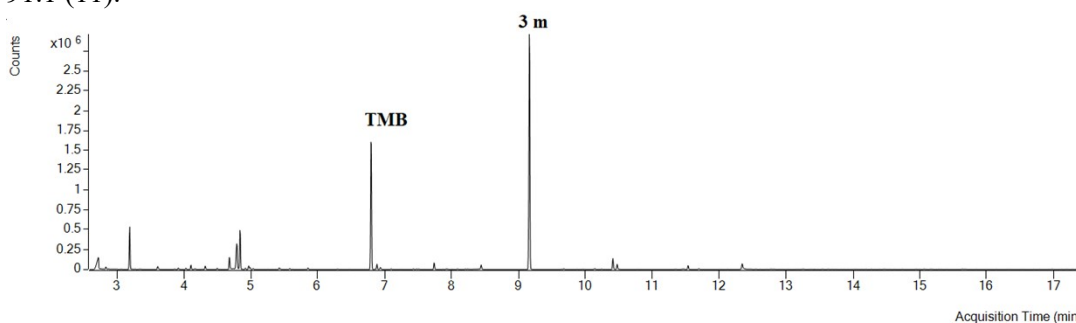


Figure S22. The above chromatogram represents the GC-trace of bioconversion using 1,2,3,4-tetrahydroquinoline and EDA as substrates. Product **3m** elutes at 9.16 min. Internal standard TMB elutes at 6.8 min.

Reaction of **1n** and EDA was carried out using the general procedure described above. GC analysis showed the product **3n** retention at 26.19 min, and TMB at 9.77 min. The remaining amount of substrate was shown at 21.43 min. MS (EI): m/z (%) = 351.1 (45), 278.1 (100).

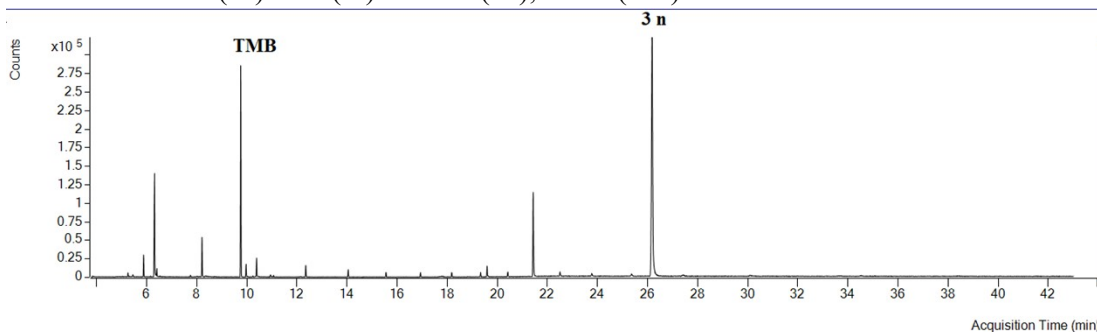


Figure S23. The above chromatogram represents the GC-trace of bioconversion using 3-(3'-amino-6'-methyl)-quinazolinone and EDA as substrates. Product **3n** elutes at 26.19 min. Internal standard TMB elutes at 9.77 min.

Reaction of **1a** and (1R,2S,5R)-2-isopropyl-5-methylcyclohexyl 2-diazoacetate was carried out using the general procedure described above. GC analysis showed the product **3o** retention at 11.56 min, and TMB at 6.8 min. There was no trace of the remaining substrate. MS (EI): m/z (%) = 289.3 (21), 151.1 (35), 106.1 (100), 77.1 (10).

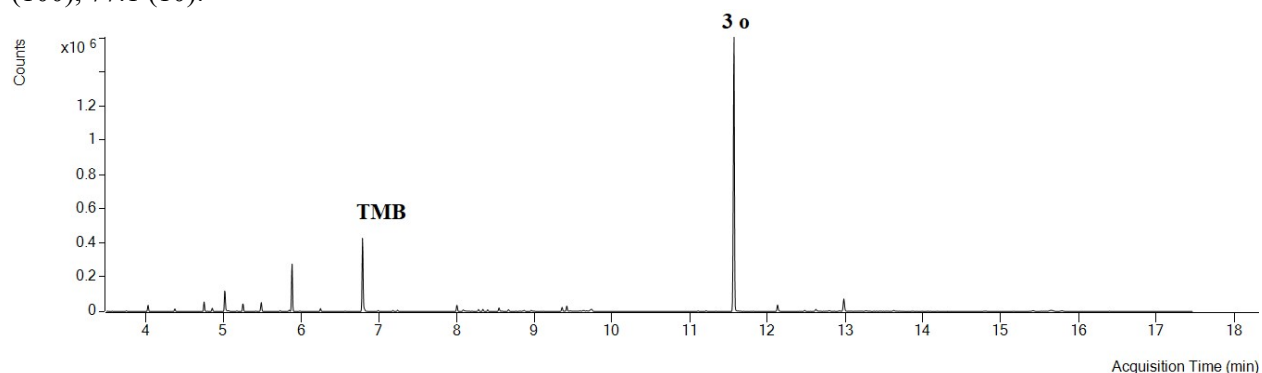
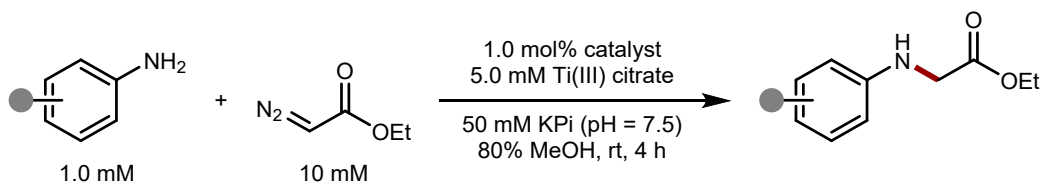
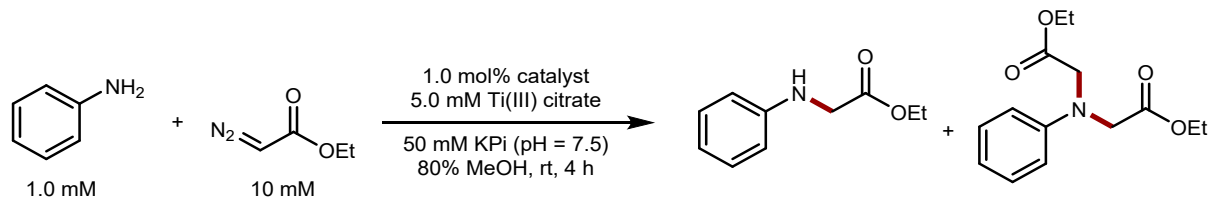


Figure S24. The above chromatogram represents the GC-trace of bioconversion using aniline and (1R,2S,5R)-2-isopropyl-5-methylcyclohexyl 2-diazoacetate as substrate. Product **3o** elutes at 11.56 min. Internal standard TMB elutes at 6.8 min.

V. Bioconversion in Methanol



Analytical scale bioconversion (800 μ L): Aniline alkylation bioconversions were set up in the wetbox under N_2 atmosphere using a 2 mL air-free Agilent glass vial. Bioconversion reactions were set up by adding aniline and ethyl diazoacetate (EDA) in 50 mM KPi-MeOH into the reaction vial, followed by the addition of catalyst (preincubated with reducing agent for 1 min) under the anaerobic condition at room temperature. The final concentration of each reagent was: 1 mM Aniline, 10 mM EDA, 1 mol% catalyst, 5 mM Ti(III) citrate, and 80% MeOH v/v. After the reaction setup, the reaction vials were agitated by end-over-end rotation for overnight at room temperature. After completion of the bioconversion, the reactions were quenched by the precipitation of enzyme using 0.1M HCl solution. The reaction mixture was collected in 2mL Eppendorf and further centrifuged to separate the organic layer. Organic components were analyzed by GC-MS.



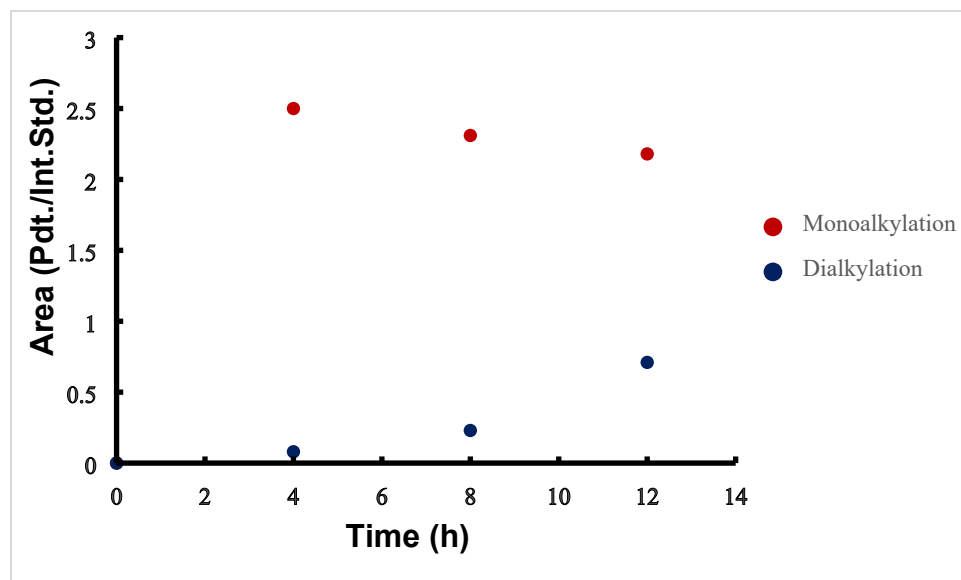


Figure S25. Time course plot for aniline alkylation with eda using MtaC as biocatalyst. Reactions were monitored over 4 h, 8 h, and 12 h for quantifying the formation of monoalkylated and dialkylated products. Reaction condition is described in the above scheme and procedures were same as analytical scale bioconversion described above.

Semi-preparative scale bioconversion (25 mL): Biotransformation on a semi-preparative scale was setup under an N₂ atmosphere in the wetbox using a 100 mL round bottom flask charged with a magnetic stir bar. Para-toluidine (50 mg, 19 mM) and 5 equivalents of EDA dissolved in MeOH-KPi were added to the flask. For the scale-up bioconversion, 0.5 mol% of MtaC preincubated with Ti(III) citrate (final concentration 5mM) was added to the reaction mixture. The flask was then sealed with the septum and kept for stirring at 150 rpm overnight. After overnight stirring, quantitative conversions were observed by GC-MS. The crude reaction mixture was quenched by the addition of 0.1 M hydrochloric acid. The precipitated enzyme was removed through celite filtration. The supernatant was then neutralized by sodium bicarbonate solution. The organic layer was then extracted and concentrated under reduced pressure. After purification by column chromatography (9:1 hexane/EtOAc), the product was obtained in a 93% yield (83 mg). Same semi-preparative scale procedure was followed for the *p*-chloroaniline (45 mg) substrate, and the product was isolated in 90% yield (68mg).

VI. Initial Rate Studies

A) Axial Mutants (H136A, D134A, T187A) MtaC Screening

For evaluating the activity of different axial variants, a general bioconversion reaction procedure was followed for all variants. Each variant reaction was set up in triplicate.

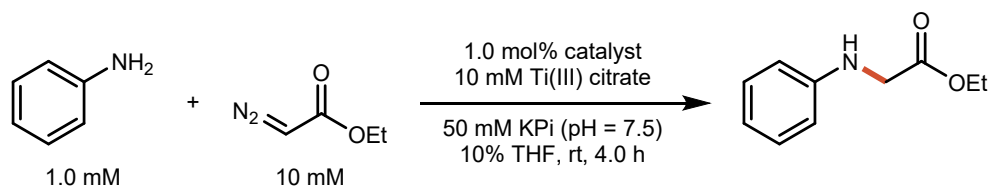


Table S3 N-alkylation reaction catalyzed by different variants of MtaC

Entry	Variants	Yield (%)
1	Parent MtaC	>99
2	T187A	65 ± 3
3	D134A	35 ± 5
4	H136A	24 ± 2

B) Initial Rate Measurements

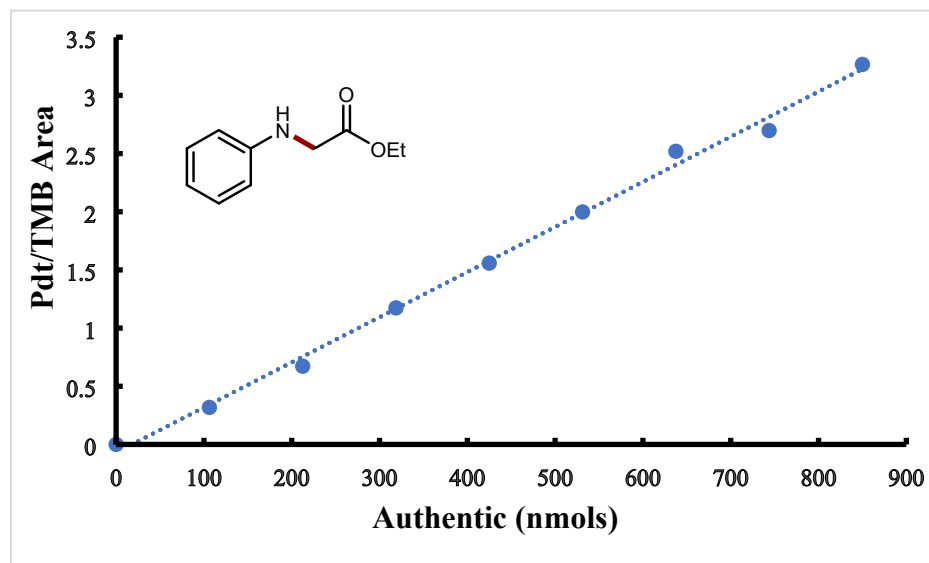
To find the rate of N-alkylation reaction using different axial mutants under the linear rate range, time-course reactions were set up using the general bioconversion reaction condition for 0-40 min (scheme 1). Reactions at each time point represent three reactions in parallel. All the triplicate reactions were quenched at the same time and the product yields were analyzed by the GC-MS (procedure described before).

Table S4 Initial rate measurement of different axial mutants of MtaC for N-alkylation reaction

Entry	Variants	Initial Rate ($\mu\text{M}/\text{min}$)
1	Parent MtaC	13.26 ± 0.13
2	T187A	6.24 ± 0.001
3	D134A	6.16 ± 0.06
4	H136A	1.63 ± 0.02

VII. GCMS Calibration Curves

The calibration curves were constructed by plotting the peak's integration ratios of 480 nmol of internal standard TMB and authentic products 1a-o in 800 μL of ethyl acetate solution. Each sample was prepared by mixing 480 nmol of internal standard with 0-850 nmol of authentic products 1a-o in 800 μL of ethyl acetate solution. All the samples were analyzed by GC-MS instruments.

**Figure S26.** Calibration curve of product 3a. Representative data points were constructed by adding 480 nmol of Internal Standard (TMB) with 0-850 nmol of authentic 3a in 800 μL of ethyl acetate solution.

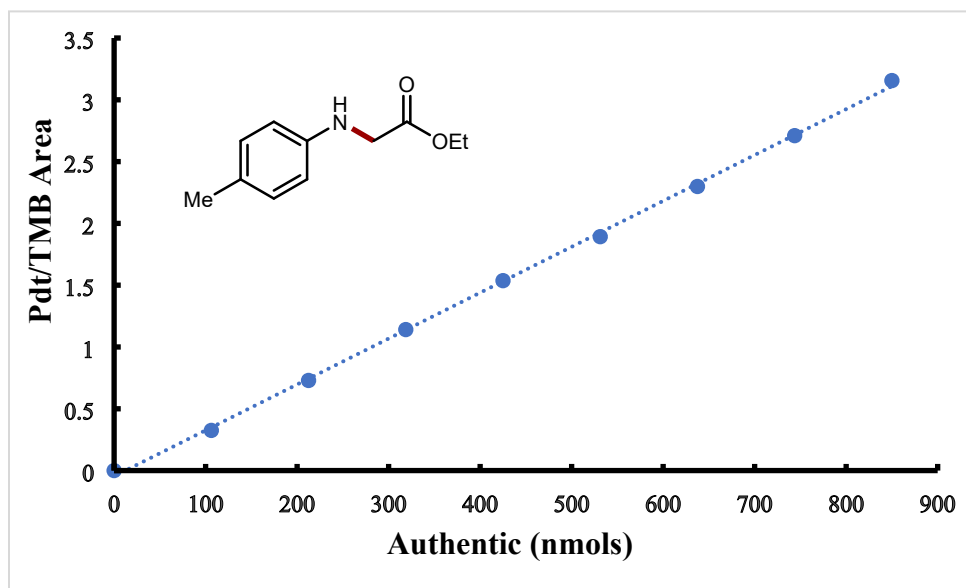


Figure S27. Calibration curve of product **3b**. Representative data points were constructed by adding 480 nmol of Internal Standard (TMB) with 0-850 nmol of authentic **3b** in 800 μ L of ethyl acetate solution.

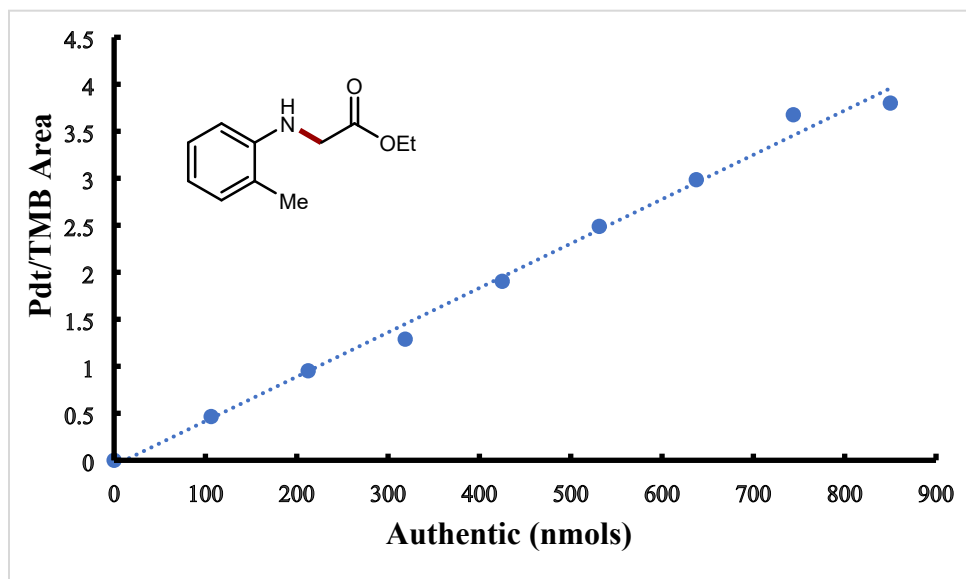


Figure S28. Calibration curve of product **3c**. Representative data points were constructed by adding 480 nmol of Internal Standard (TMB) with 0-850 nmol of authentic **3c** in 800 μ L of ethyl acetate solution.

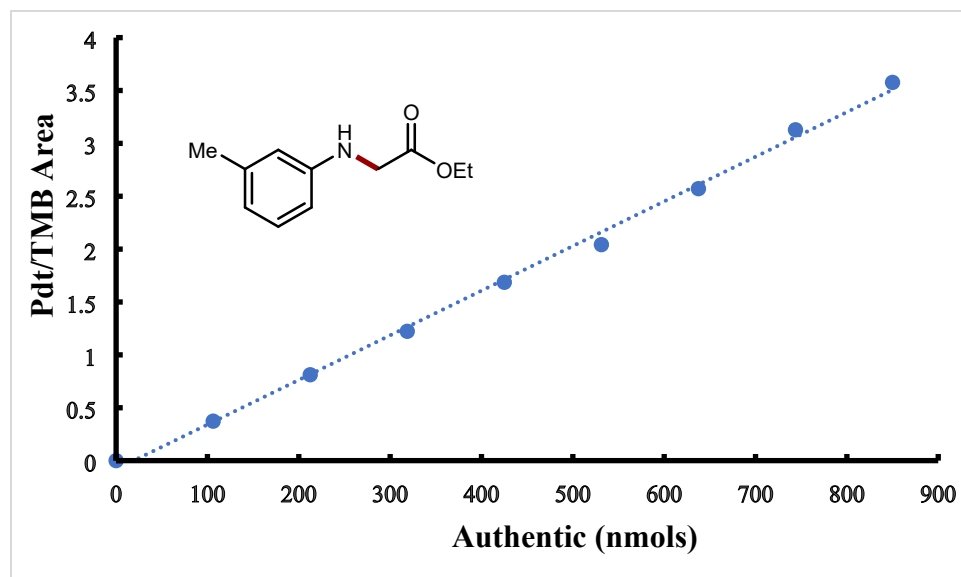


Figure S29. Calibration curve of product **3d**. Representative data points were constructed by adding 480 nmol of Internal Standard (TMB) with 0-850 nmol of authentic **3d** in 800 μ L of ethyl acetate solution.

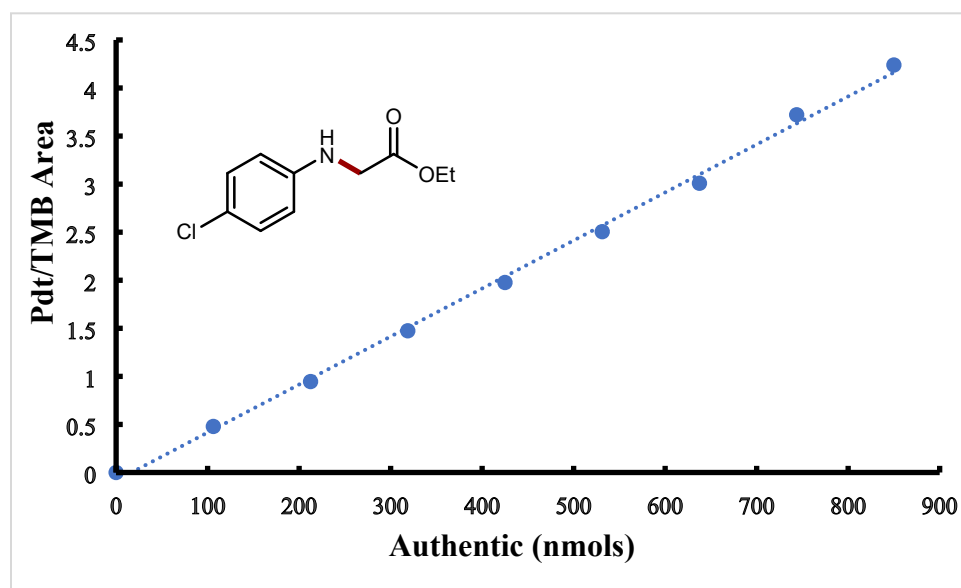


Figure S30. Calibration curve of product **3e**. Representative data points were constructed by adding 480 nmol of Internal Standard (TMB) with 0-850 nmol of authentic **3e** in 800 μ L of ethyl acetate solution.

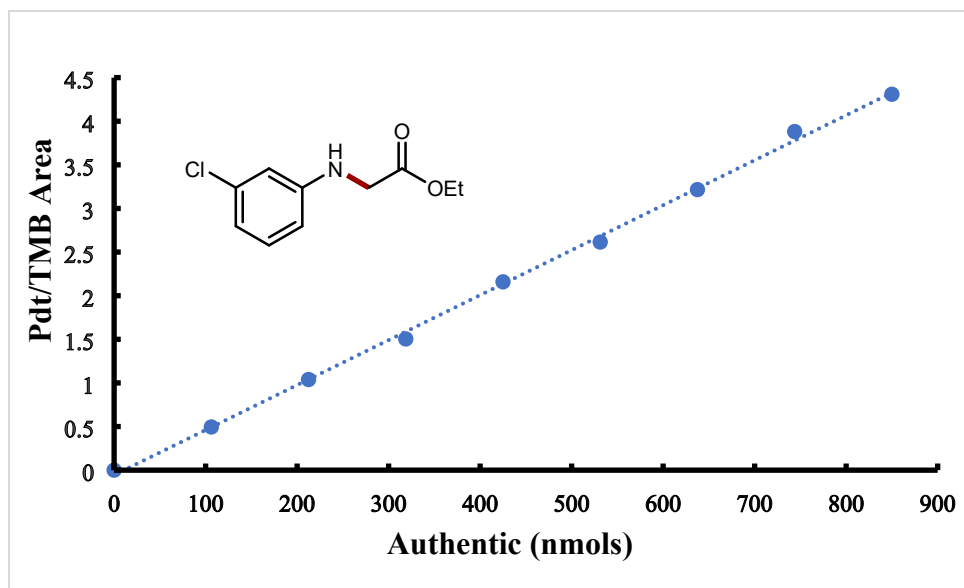


Figure S31. Calibration curve of product **3f**. Representative data points were constructed by adding 480 nmol of Internal Standard (TMB) with 0-850 nmol of authentic **3f** in 800 μ L of ethyl acetate solution.

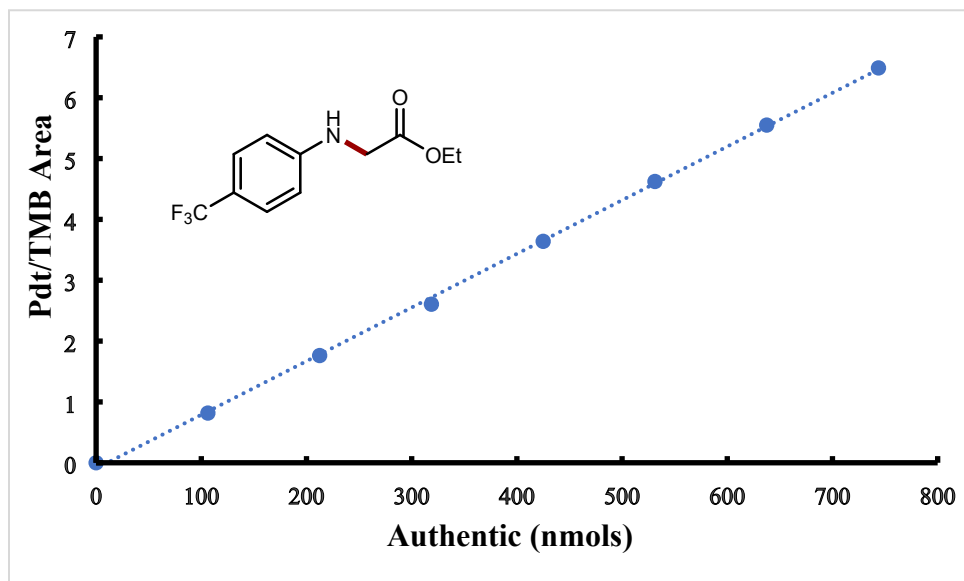


Figure S32. Calibration curve of product **3g**. Representative data points were constructed by adding 480 nmol of Internal Standard (TMB) with 0-850 nmol of authentic **3g** in 800 μ L of ethyl acetate solution.

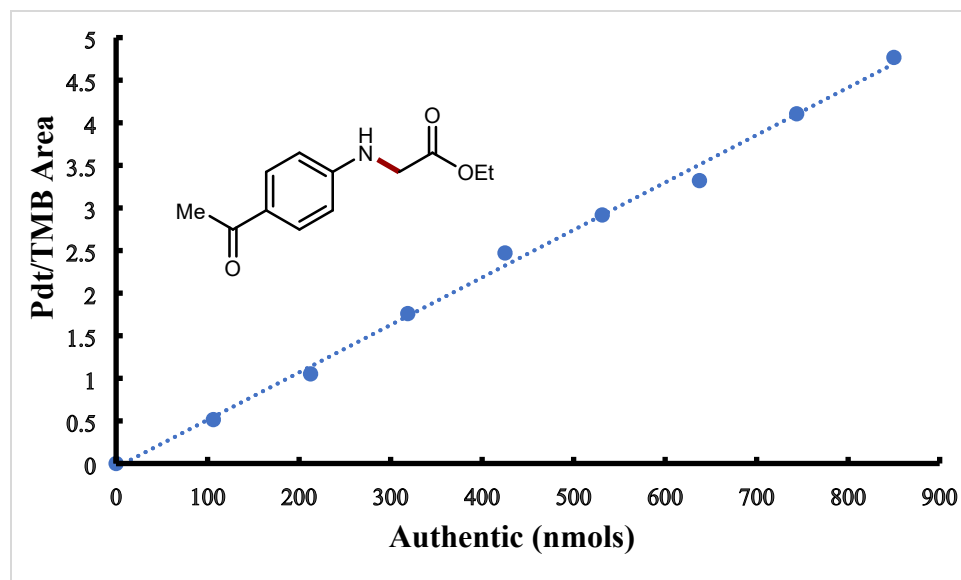


Figure S33. Calibration curve of product **3h**. Representative data points were constructed by adding 480 nmol of Internal Standard (TMB) with 0-850 nmol of authentic **3h** in 800 μ L of ethyl acetate solution.

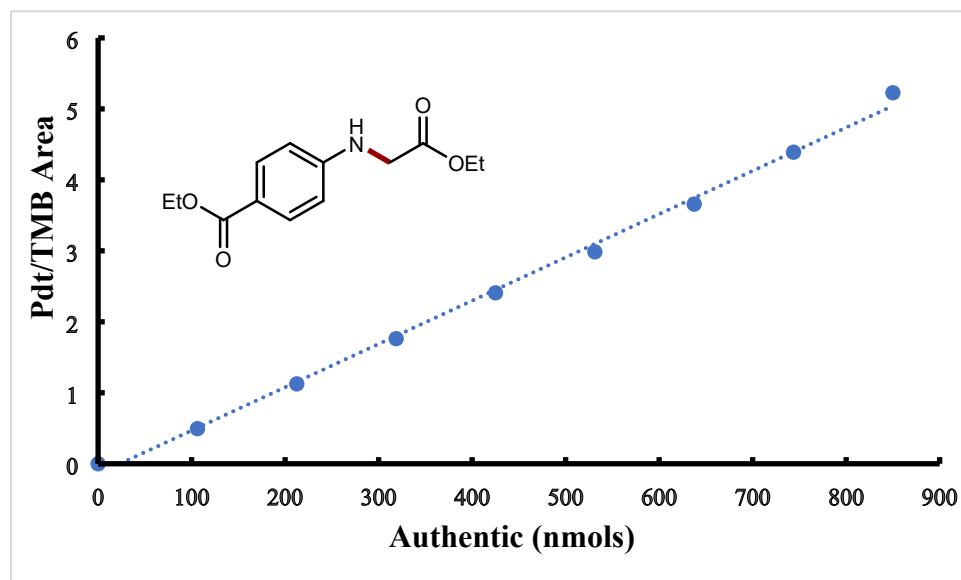


Figure S34. Calibration curve of product **3i**. Representative data points were constructed by adding 480 nmol of Internal Standard (TMB) with 0-850 nmol of authentic **3i** in 800 μ L of ethyl acetate solution.

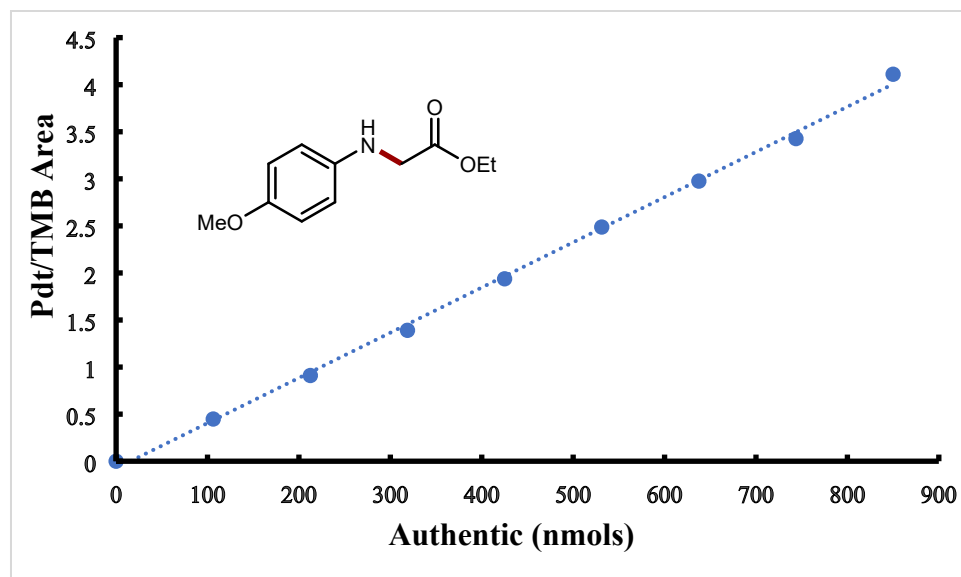


Figure S35. Calibration curve of product **3j**. Representative data points were constructed by adding 480 nmol of Internal Standard (TMB) with 0-850 nmol of authentic **3j** in 800 μ L of ethyl acetate solution.

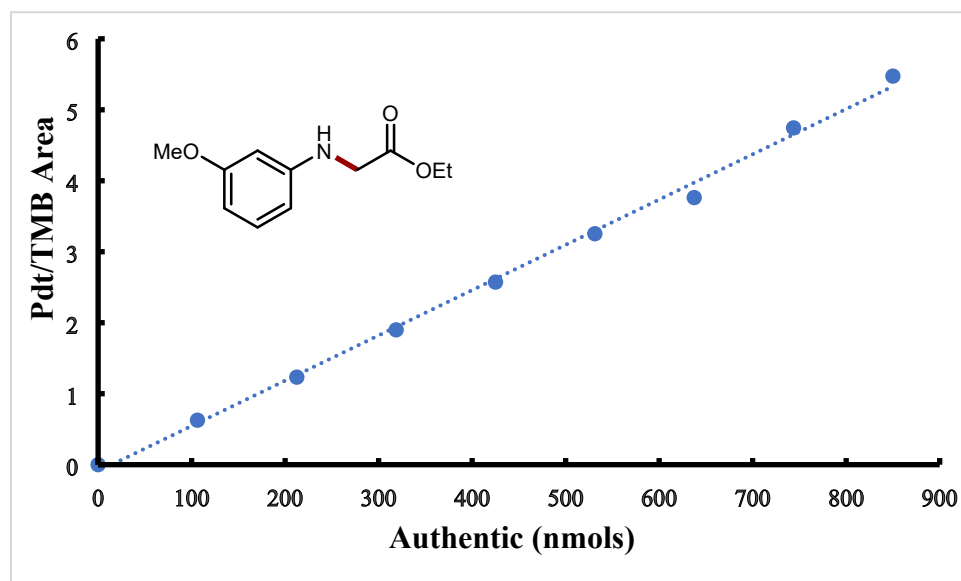


Figure S36. Calibration curve of product **3k**. Representative data points were constructed by adding 480 nmol of Internal Standard (TMB) with 0-850 nmol of authentic **3k** in 800 μ L of ethyl acetate solution.

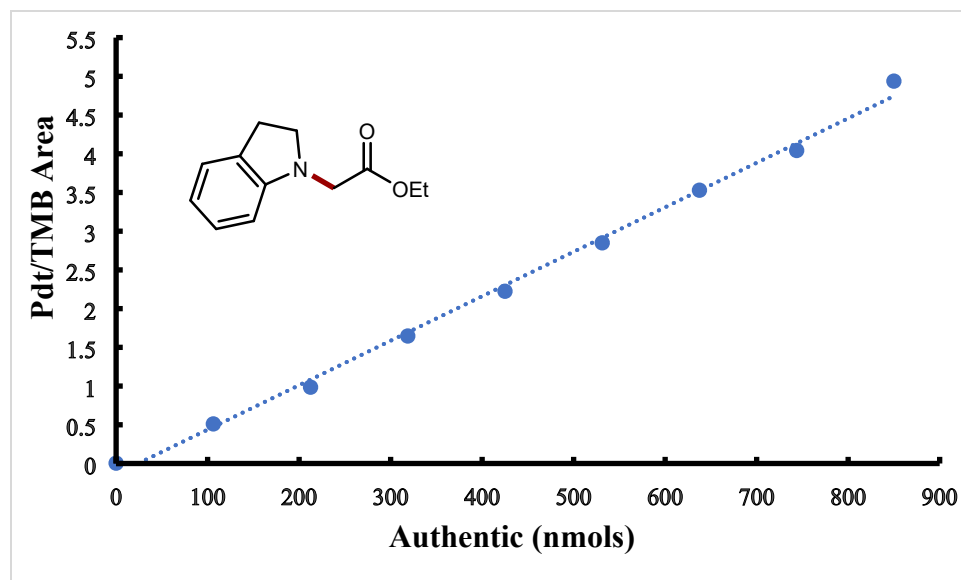


Figure S37. Calibration curve of product **3l**. Representative data points were constructed by adding 480 nmol of Internal Standard (TMB) with 0-850 nmol of authentic **3l** in 800 μ L of ethyl acetate solution.

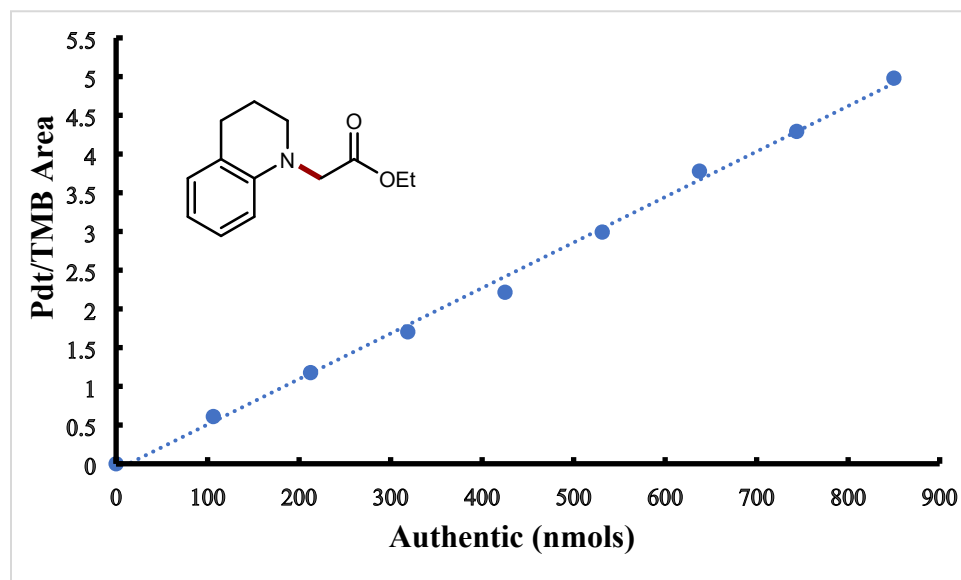


Figure S38. Calibration curve of product **3m**. Representative data points were constructed by adding 480 nmol of Internal Standard (TMB) with 0-850 nmol of authentic **3m** in 800 μ L of ethyl acetate solution.

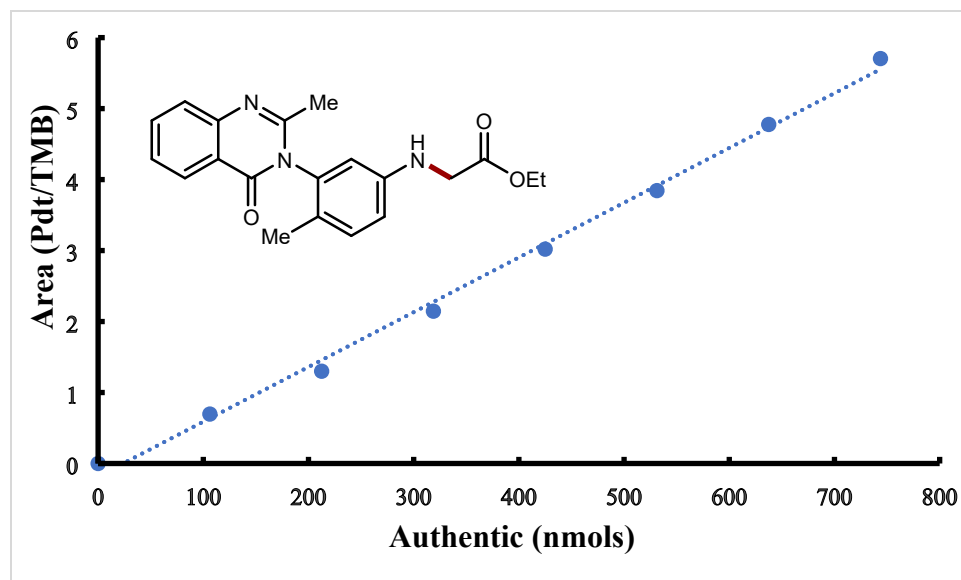


Figure S39. Calibration curve of product **3n**. Representative data points were constructed by adding 480 nmol of Internal Standard (TMB) with 0-850 nmol of authentic **3n** in 800 μ L of ethyl acetate solution.

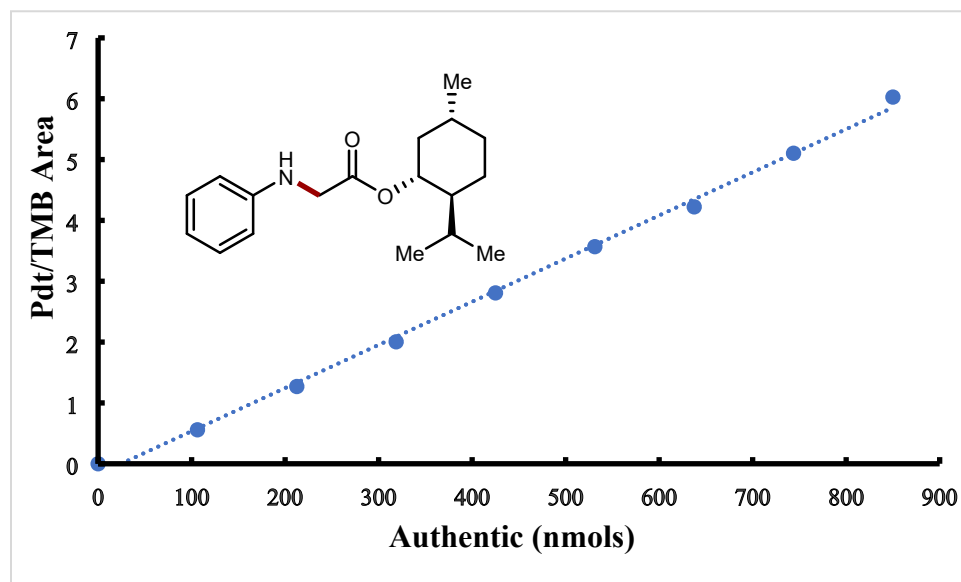
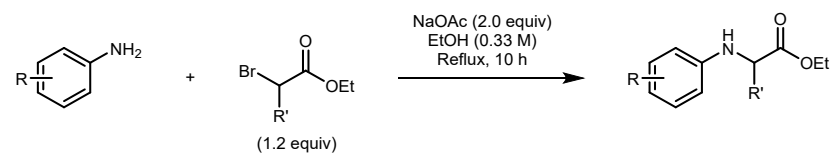
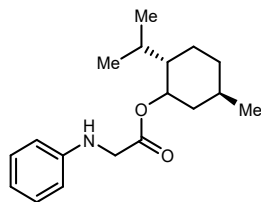


Figure S40. Calibration curve of product **3o**. Representative data points were constructed by adding 480 nmol of Internal Standard (TMB) with 0-850 nmol of authentic **3o** in 800 μ L of ethyl acetate solution.

VIII. Synthetic Procedures

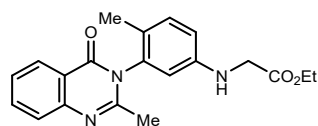


General procedure for *N*-aryl glycine derivatives synthesis⁵: A mixture of aniline (3.0 mmol, 1.0 equiv), α -bromoester (3.6 mmol, 1.2 equiv) and anhydrous sodium acetate (NaOAc, 6.0 mmol, 2.0 equiv) in 9.0 mL ethanol was refluxed for 10 hours. The mixture was then cooled down to room temperature and filtered through celite. The celite was washed by dichloromethane and the combined organic layer was evaporated to remove the volatile. The crude residue was then purified by column on silica gel with hexane and ethyl acetate to the desired *N*-aryl glycine derivatives.



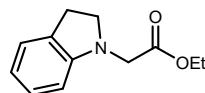
¹H NMR (500 MHz, CDCl₃) δ 7.11 (dd, J = 8.6, 7.3 Hz, 2H), 6.67 (t, J = 7.3 Hz, 1H), 6.53 (d, J = 7.5 Hz, 2H), 4.71 (td, J = 10.9, 4.4 Hz, 1H), 4.23 (s, 1H), 3.80 (s, 2H), 1.97 – 1.89 (m, 1H), 1.78 – 1.66 (m, 1H), 1.66 – 1.56 (m, 2H), 1.49 – 1.36 (m, 1H), 1.36 – 1.27 (m, 1H), 1.03 – 0.89 (m, 2H), 0.83 (d, J = 6.6 Hz, 3H), 0.80 (d, J = 7.1 Hz, 3H), 0.66 (d, J = 6.9 Hz, 3H).

¹³C NMR (126 MHz, CDCl₃) δ 170.8, 147.1, 129.3, 118.2, 113.0, 75.4, 47.0, 46.1, 40.9, 34.2, 31.4, 26.3, 23.4, 22.0, 20.8, 16.3.



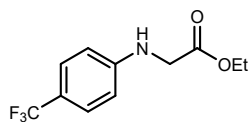
¹H NMR (500 MHz, CDCl₃) δ 8.27 (d, J = 7.2 Hz, 1H), 7.75 (t, J = 7.5 Hz, 1H), 7.66 (d, J = 8.2 Hz, 1H), 7.45 (t, J = 7.6 Hz, 1H), 7.17 (d, J = 8.3 Hz, 1H), 6.65 (dd, J = 8.3, 2.5 Hz, 1H), 6.38 (d, J = 2.5 Hz, 1H), 4.41 (s, 1H), 4.22 (q, J = 7.1 Hz, 2H), 3.91 – 3.82 (m, 2H), 2.21 (s, 3H), 1.97 (s, 3H), 1.27 (t, J = 7.1 Hz, 4H).

¹³C NMR (126 MHz, CDCl₃) δ 170.8, 161.6, 154.6, 147.7, 146.8, 137.5, 134.5, 132.2, 127.1, 126.8, 126.5, 123.9, 120.8, 114.5, 111.8, 61.4, 45.9, 23.7, 16.4, 14.2.



¹H NMR (500 MHz, CDCl₃) δ 7.02 (d, J = 7.3 Hz, 1H), 6.98 (t, J = 7.7 Hz, 1H), 6.61 (t, J = 7.4 Hz, 1H), 6.34 (d, J = 7.8 Hz, 1H), 4.13 (q, J = 7.2 Hz, 2H), 3.81 (s, 2H), 3.47 (t, J = 8.4 Hz, 2H), 2.96 (t, J = 8.4 Hz, 2H), 1.28 – 1.17 (m, 5H).

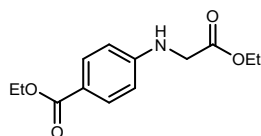
¹³C NMR (126 MHz, CDCl₃) δ 170.3, 151.3, 129.7, 127.3, 124.6, 118.2, 106.7, 60.9, 53.9, 50.6, 28.7, 14.3.



¹H NMR (500 MHz, CDCl₃) δ 7.35 (d, *J* = 8.3 Hz, 2H), 6.54 (d, *J* = 8.2 Hz, 2H), 4.56 (s, 1H), 4.19 (q, *J* = 7.2 Hz, 2H), 3.85 (d, *J* = 5.3 Hz, 2H), 1.24 (t, *J* = 7.2 Hz, 3H).

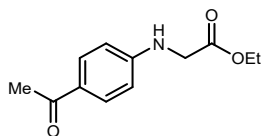
¹³C NMR (126 MHz, CDCl₃) δ 170.5, 149.4, 126.7 (q, *J* = 3.8 Hz), 124.9 (q, *J* = 270.5 Hz), 119.7 (q, *J* = 32.7 Hz), 112.1, 61.7, 45.2, 14.2.

¹⁹F NMR (471 MHz, CDCl₃) δ -61.12 (s, 3F).



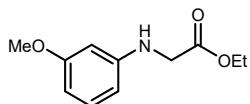
¹H NMR (500 MHz, CDCl₃) δ 7.82 (d, *J* = 8.3 Hz, 2H), 6.50 (d, *J* = 8.3 Hz, 2H), 4.25 (q, *J* = 7.3 Hz, 2H), 4.20 (q, *J* = 7.1 Hz, 2H), 3.87 (d, *J* = 5.1 Hz, 2H), 1.29 (t, *J* = 7.1 Hz, 3H), 1.24 (t, *J* = 7.1 Hz, 3H).

¹³C NMR (126 MHz, CDCl₃) δ 170.4, 166.8, 150.5, 131.6, 119.7, 111.8, 61.7, 60.3, 45.1, 14.5, 14.2.



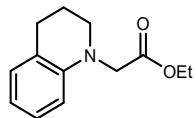
¹H NMR (500 MHz, CDCl₃) δ 7.76 (d, *J* = 8.8 Hz, 2H), 6.49 (d, *J* = 8.7 Hz, 2H), 4.84 (s, 1H), 4.18 (q, *J* = 7.1 Hz, 2H), 3.87 (d, *J* = 5.2 Hz, 2H), 2.42 (s, 3H), 1.23 (t, *J* = 7.1 Hz, 3H).

¹³C NMR (126 MHz, CDCl₃) δ 196.5, 170.3, 150.9, 130.8, 127.4, 111.7, 61.7, 45.0, 26.1, 14.2.



¹H NMR (500 MHz, CDCl₃) δ 7.03 (t, *J* = 8.1 Hz, 1H), 6.25 (d, *J* = 7.9 Hz, 1H), 6.17 (d, *J* = 8.4 Hz, 1H), 6.09 (s, 1H), 4.24 (s, 1H), 4.18 (q, *J* = 7.2 Hz, 2H), 3.82 (d, *J* = 5.2 Hz, 2H), 3.71 (s, 3H), 1.23 (t, *J* = 7.1 Hz, 3H).

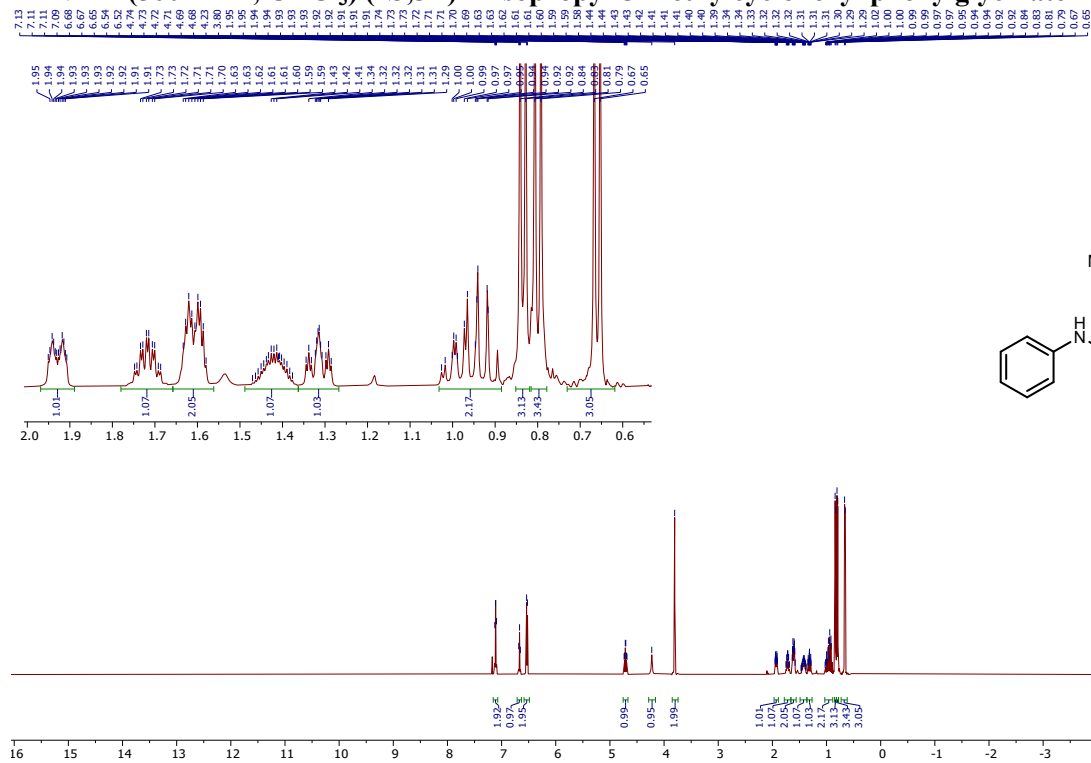
¹³C NMR (126 MHz, CDCl₃) δ 171.1, 160.8, 148.4, 130.1, 106.0, 103.3, 99.1, 61.4, 55.1, 45.8, 14.2.



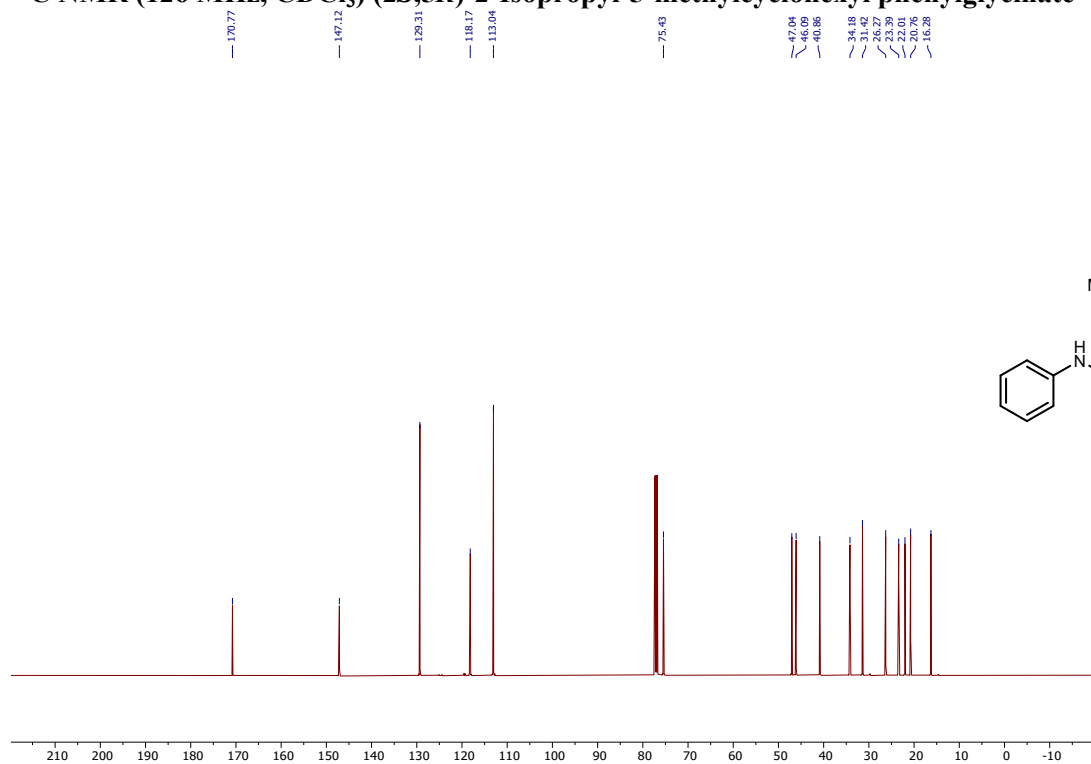
¹H NMR (400 MHz, cdcl₃) δ 6.60 (t, *J* = 7.3 Hz, 1H), 6.40 (d, *J* = 8.2 Hz, 1H), 4.17 (q, *J* = 7.1 Hz, 2H), 3.97 (s, 2H), 3.39 (t, *J* = 5.7 Hz, 2H), 2.77 (t, *J* = 6.4 Hz, 2H), 1.98 (p, *J* = 6.2 Hz, 2H), 1.23 (d, *J* = 7.1 Hz, 3H).

¹³C NMR (101 MHz, cdcl₃) δ 171.1, 144.7, 129.1, 127.0, 122.8, 116.7, 110.3, 60.8, 53.2, 50.6, 27.9, 22.3, 14.2.

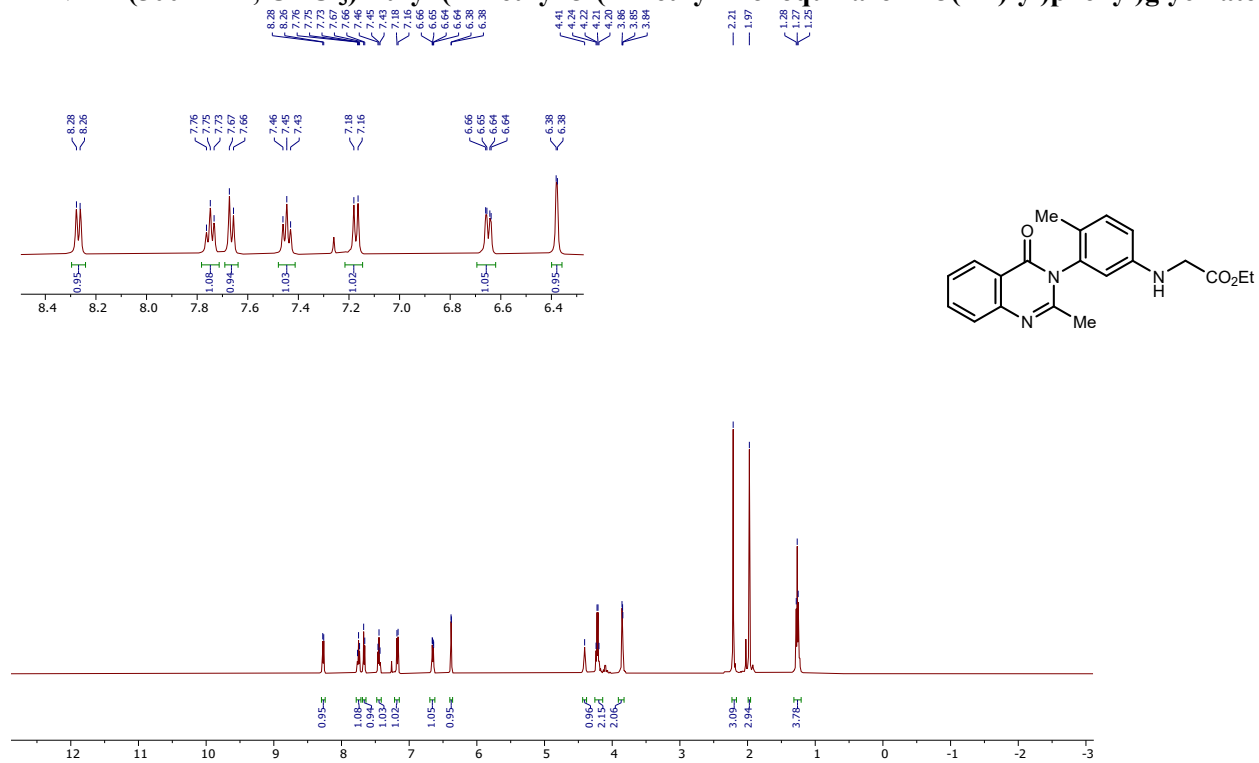
¹H NMR (500 MHz, CDCl₃) (2*S*,5*R*)-2-Isopropyl-5-methylcyclohexyl phenylglycinate



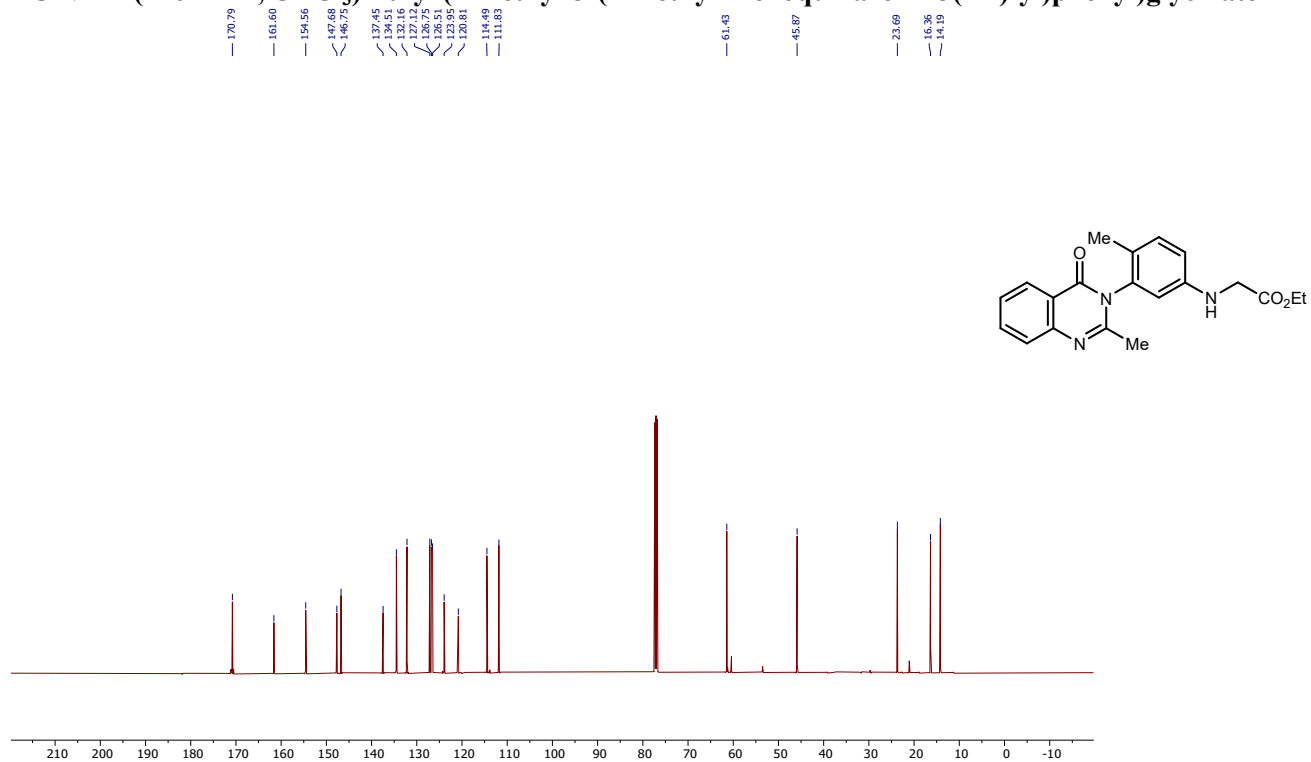
¹³C NMR (126 MHz, CDCl₃) (2*S*,5*R*)-2-Isopropyl-5-methylcyclohexyl phenylglycinate



¹H NMR (500 MHz, CDCl₃) Ethyl (4-methyl-3-(2-methyl-4-oxoquinazolin-3(4H)-yl)phenyl)glycinate

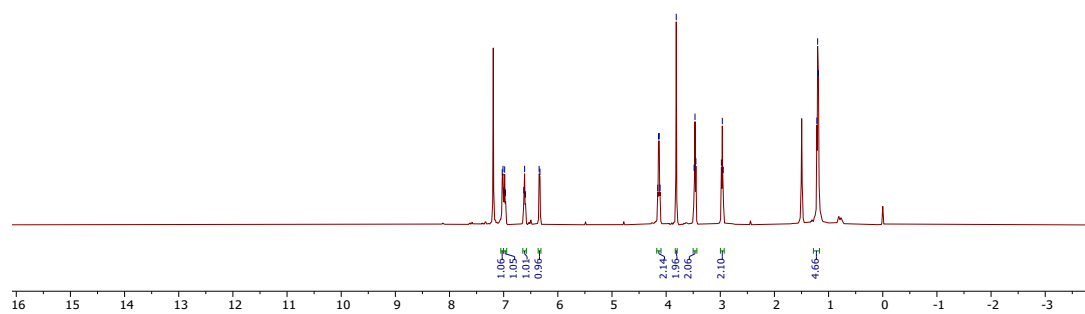
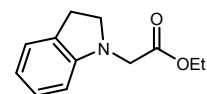


¹³C NMR (126 MHz, CDCl₃) Ethyl (4-methyl-3-(2-methyl-4-oxoquinazolin-3(4H)-yl)phenyl)glycinate



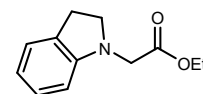
¹H NMR (500 MHz, CDCl₃) Ethyl 2-(indolin-1-yl)acetate

7.03
7.00
6.98
6.97
6.64
6.60
6.35
6.33
4.16
4.14
4.13
4.12
3.81
3.48
3.47
2.98
2.96
2.95
1.22
1.20
1.19

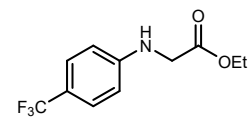
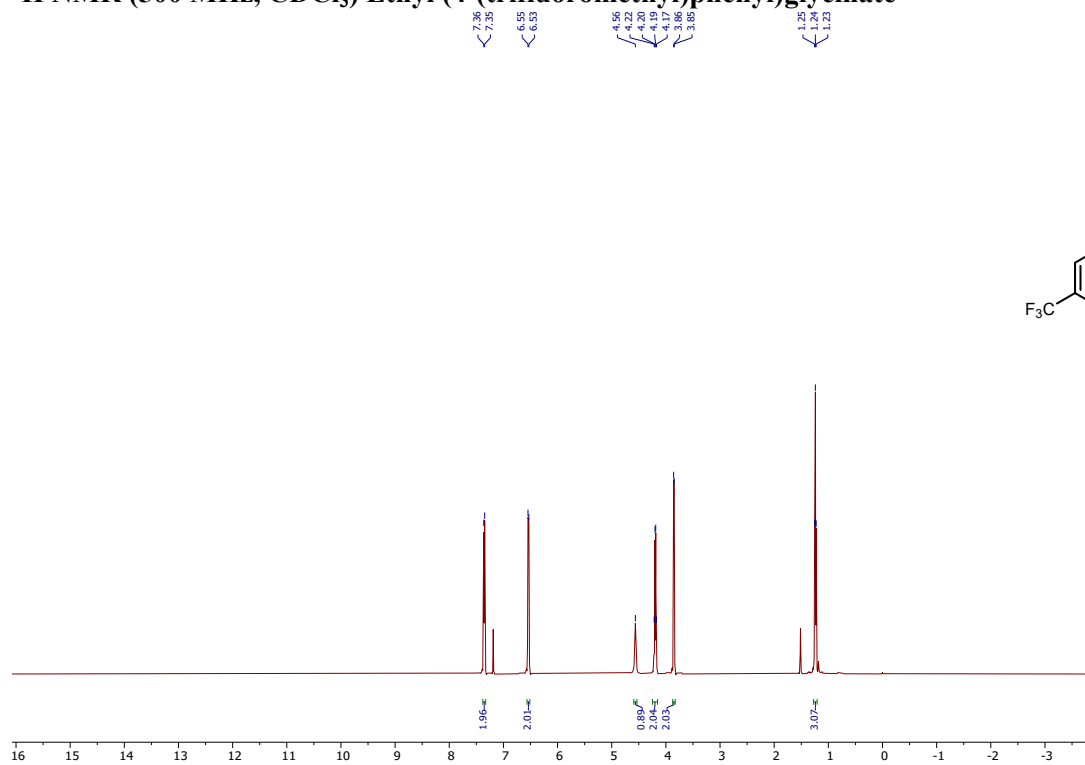


¹³C NMR (126 MHz, CDCl₃) Ethyl 2-(indolin-1-yl)acetate

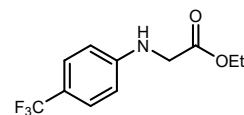
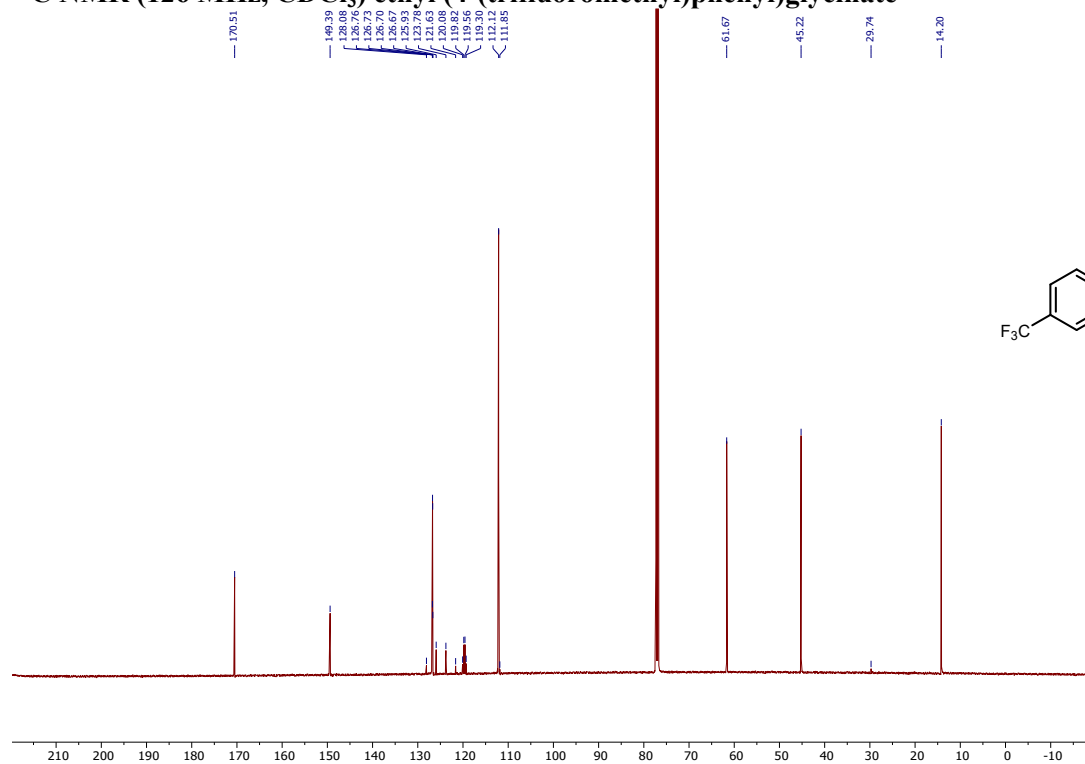
170.33
151.32
129.73
128.58
118.21
106.65
60.92
53.86
50.65
28.67
14.27



¹H NMR (500 MHz, CDCl₃) Ethyl (4-(trifluoromethyl)phenyl)glycinate

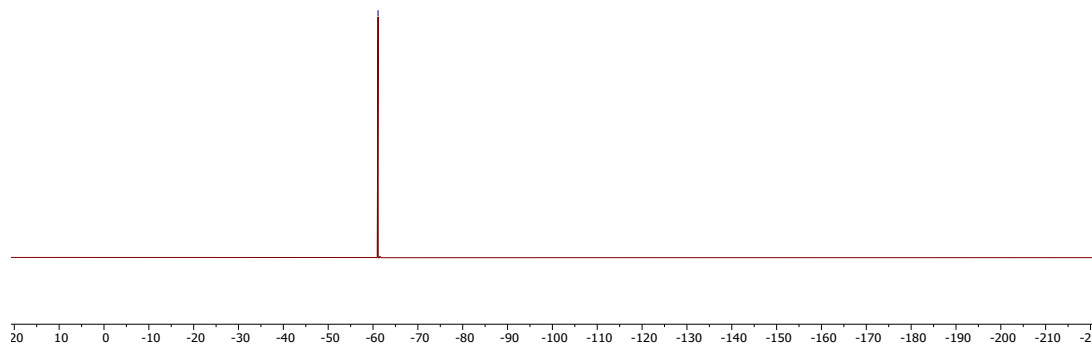
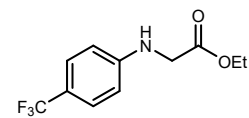


¹³C NMR (126 MHz, CDCl₃) ethyl (4-(trifluoromethyl)phenyl)glycinate

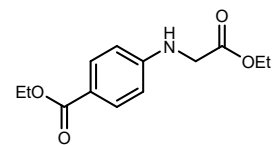
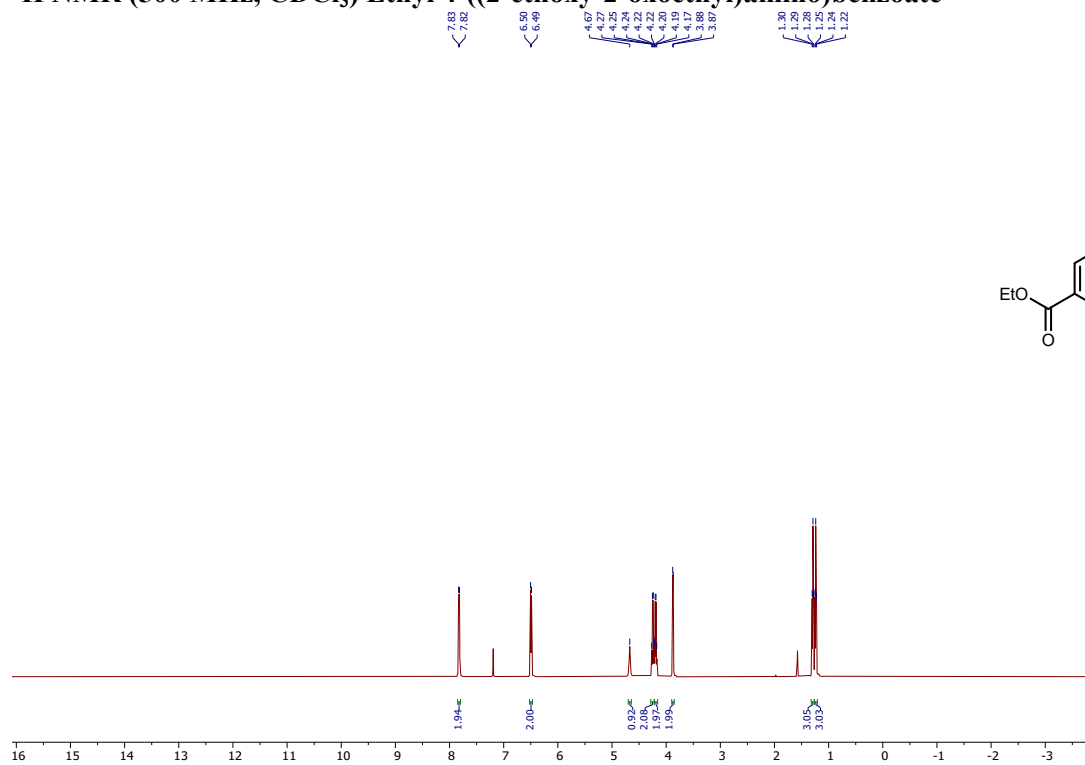


^{19}F NMR (471 MHz, CDCl_3) Ethyl (4-(trifluoromethyl)phenyl)glycinate

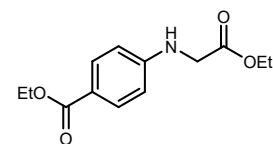
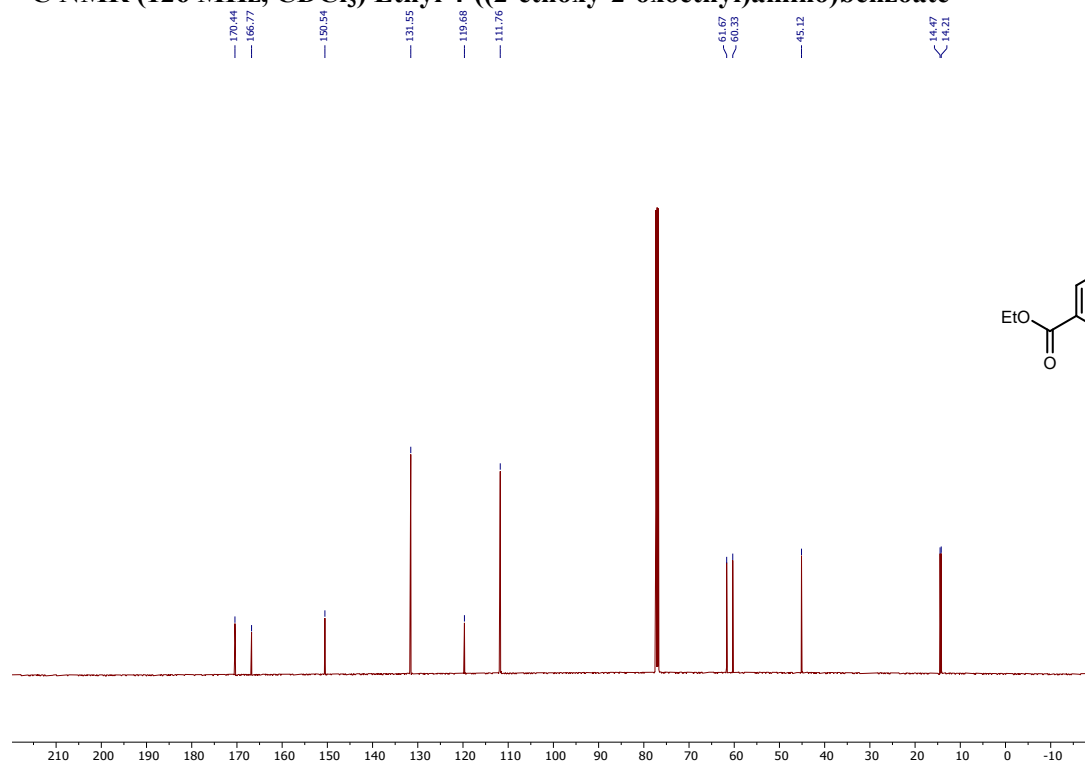
— 61.12



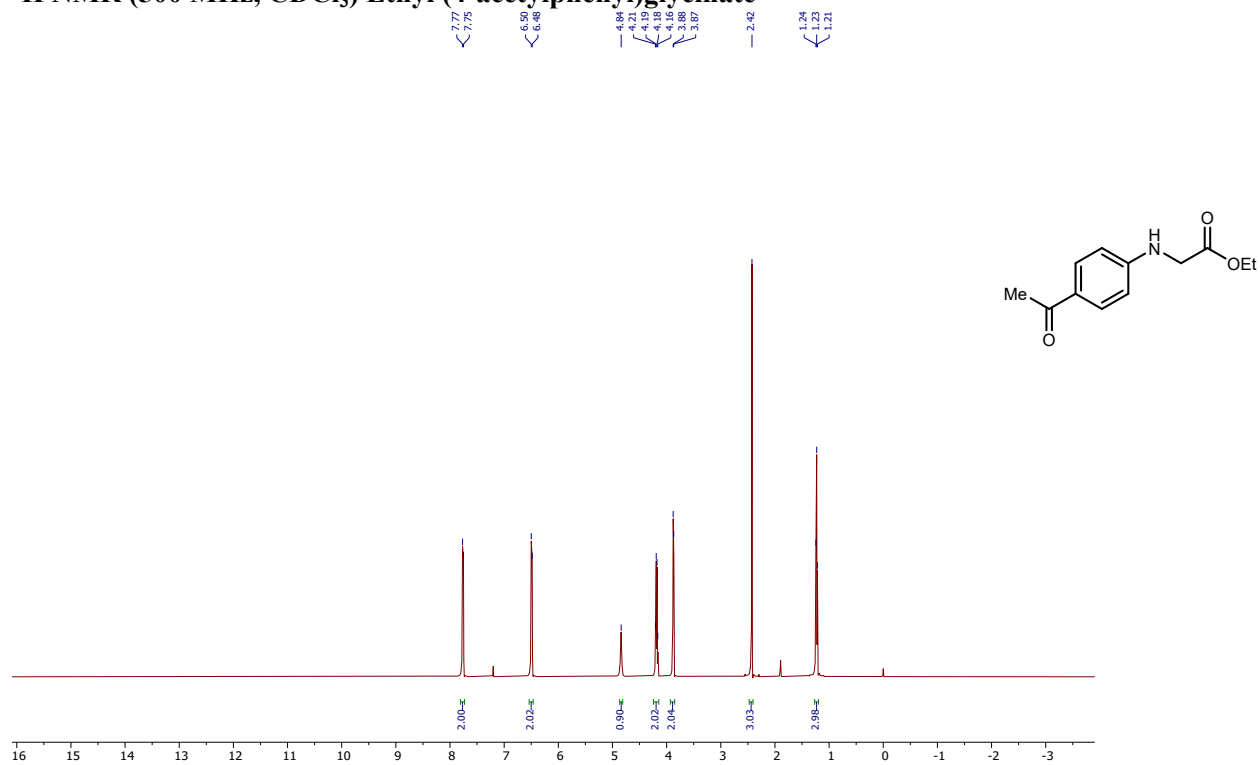
¹H NMR (500 MHz, CDCl₃) Ethyl 4-((2-ethoxy-2-oxoethyl)amino)benzoate



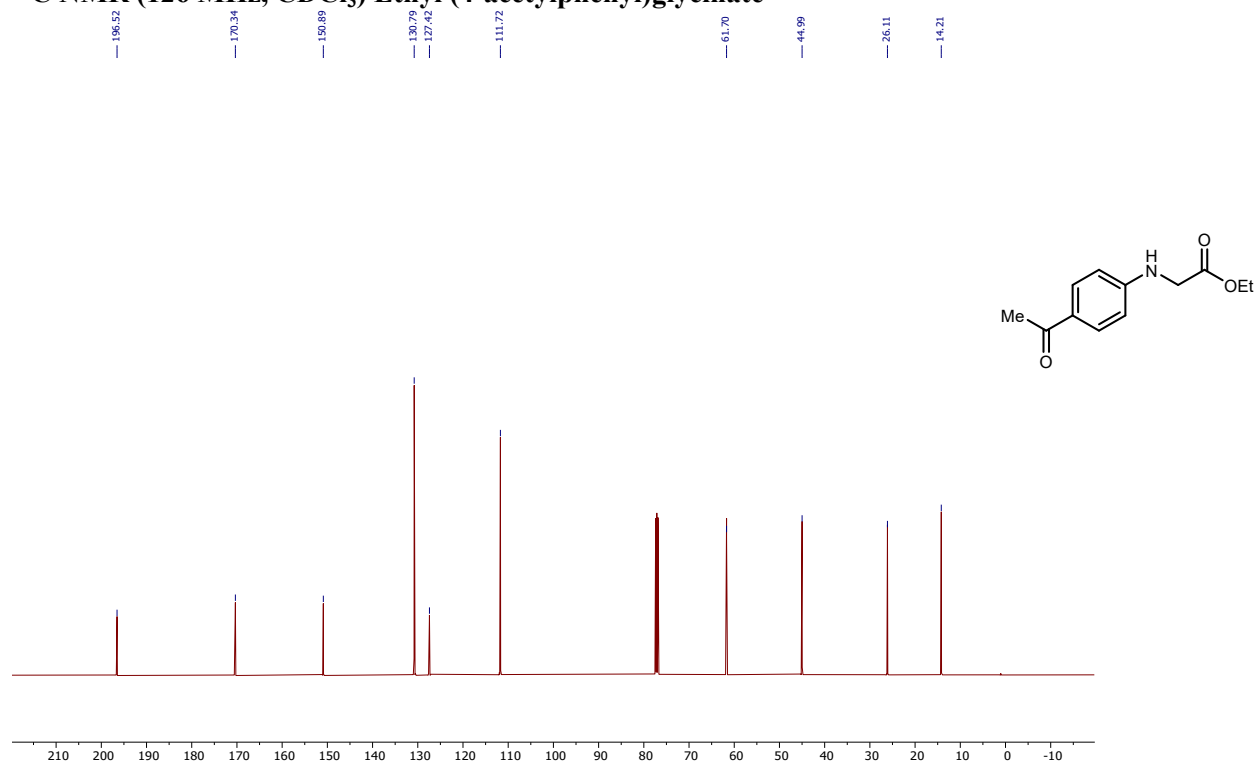
¹³C NMR (126 MHz, CDCl₃) Ethyl 4-((2-ethoxy-2-oxoethyl)amino)benzoate



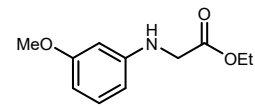
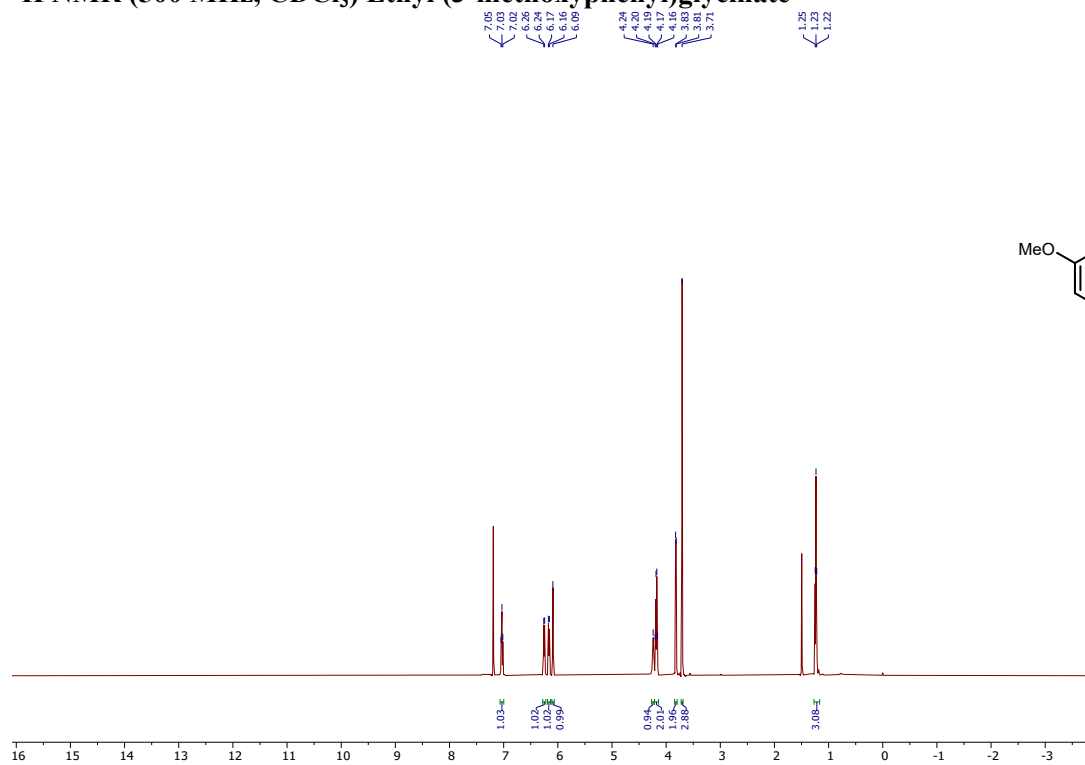
¹H NMR (500 MHz, CDCl₃) Ethyl (4-acetylphenyl)glycinate



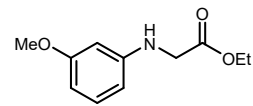
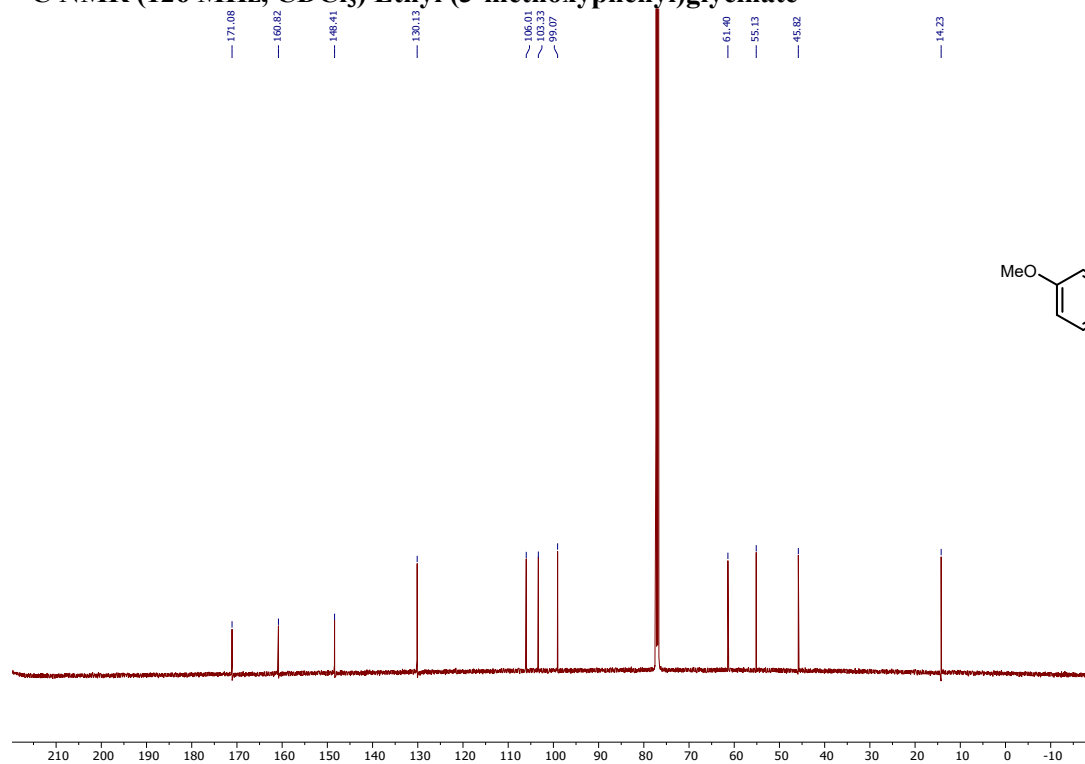
¹³C NMR (126 MHz, CDCl₃) Ethyl (4-acetylphenyl)glycinate



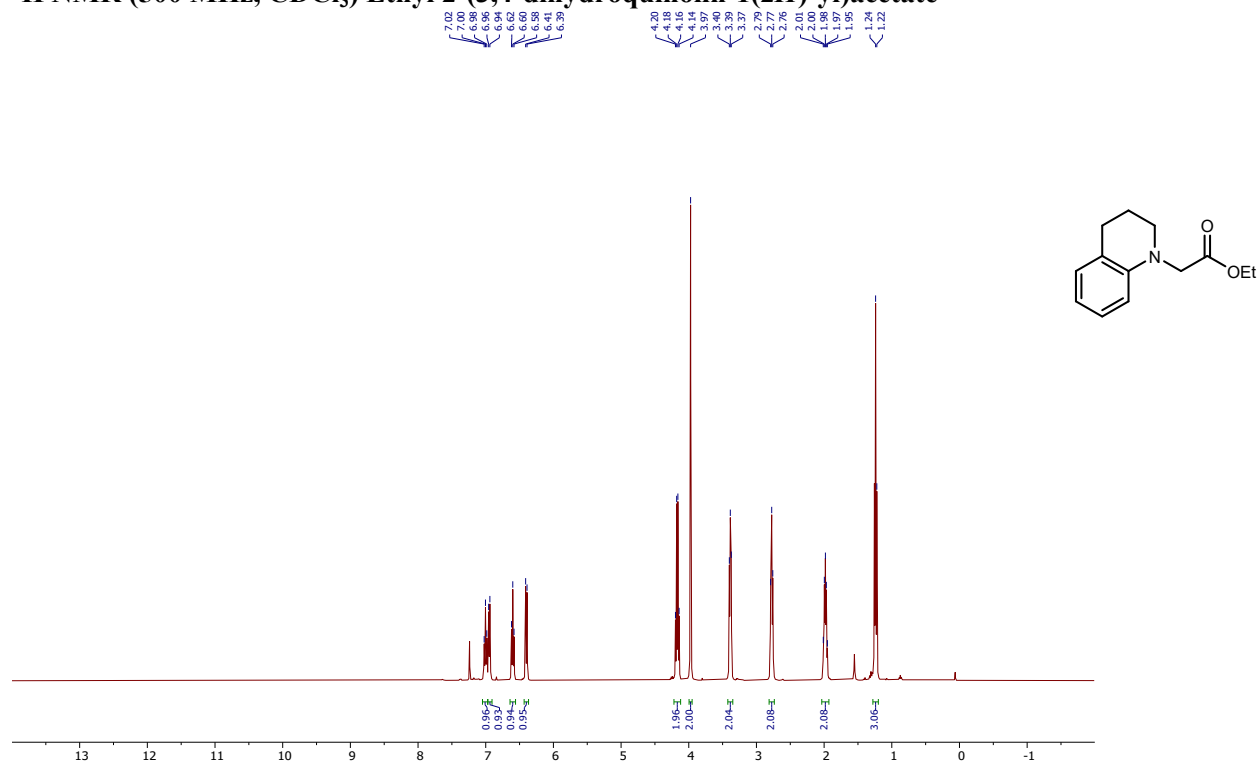
¹H NMR (500 MHz, CDCl₃) Ethyl (3-methoxyphenyl)glycinate



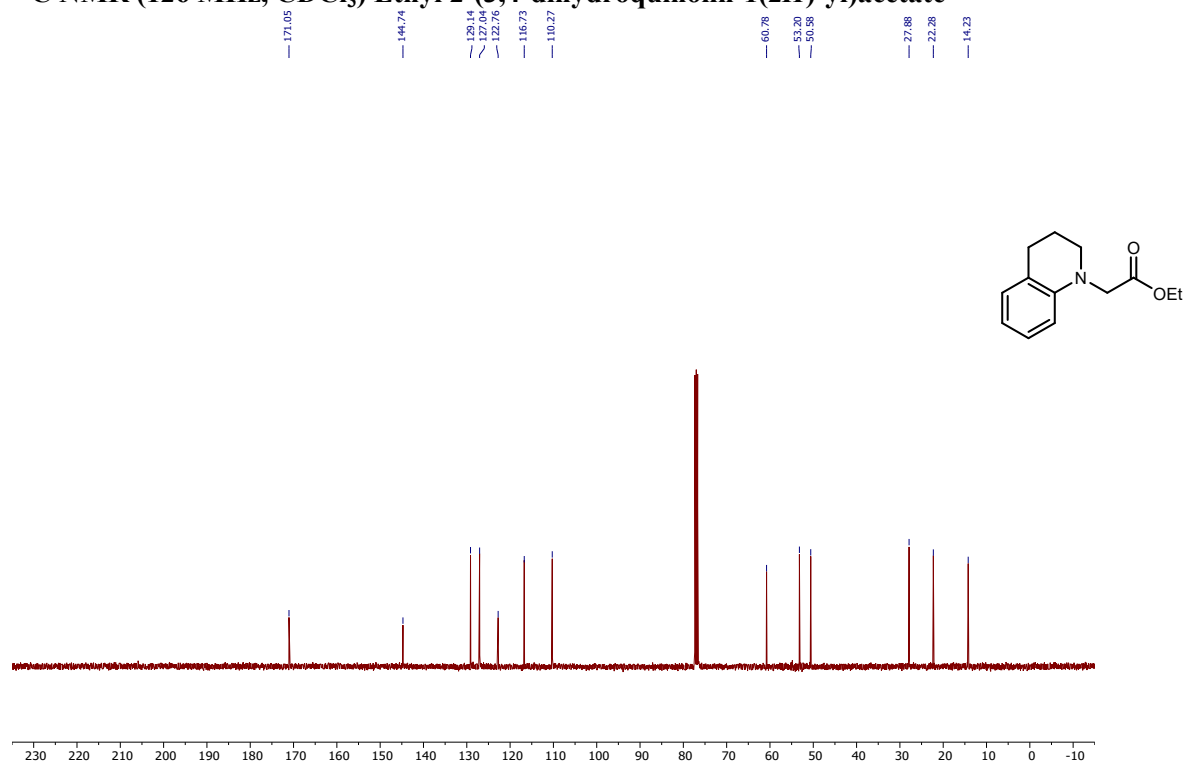
¹³C NMR (126 MHz, CDCl₃) Ethyl (3-methoxyphenyl)glycinate



¹H NMR (500 MHz, CDCl₃) Ethyl 2-(3,4-dihydroquinolin-1(2H)-yl)acetate

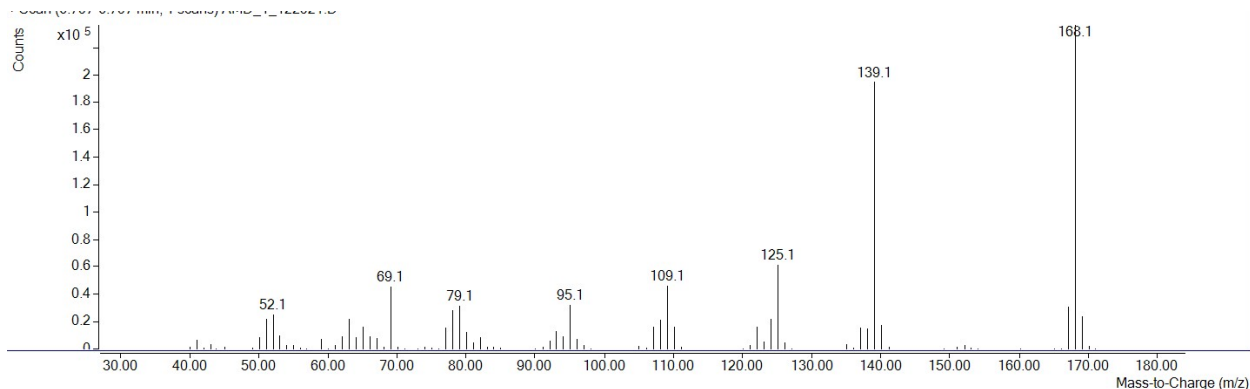


¹³C NMR (126 MHz, CDCl₃) Ethyl 2-(3,4-dihydroquinolin-1(2H)-yl)acetate

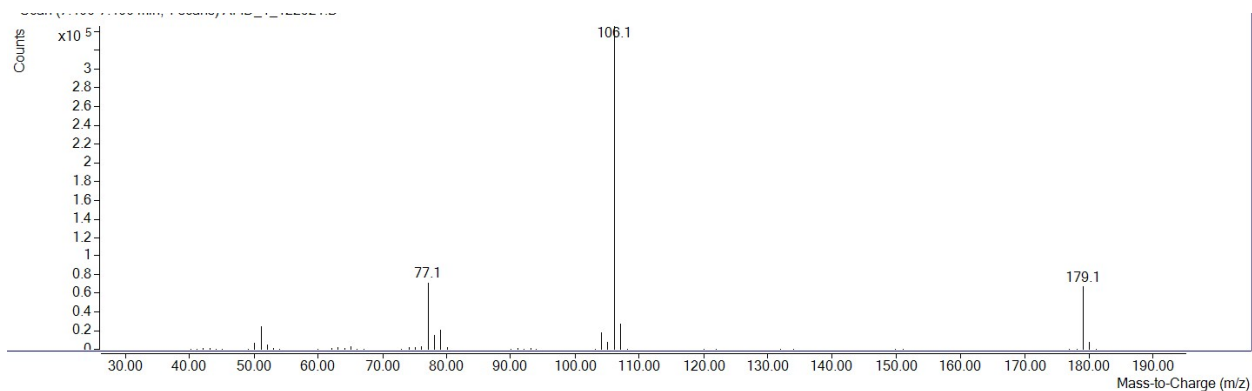


IX. Mass Spectra

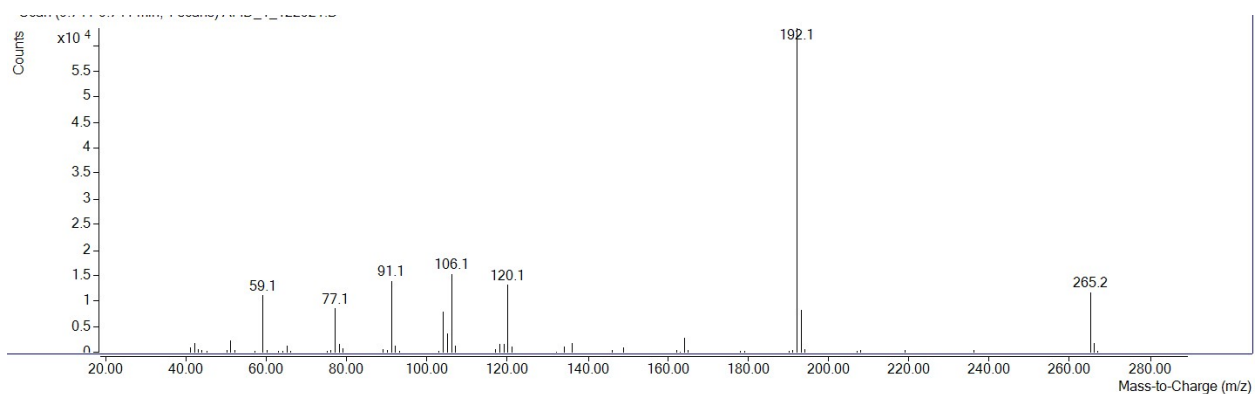
Mass spectra (MS) for internal standard (TMB)



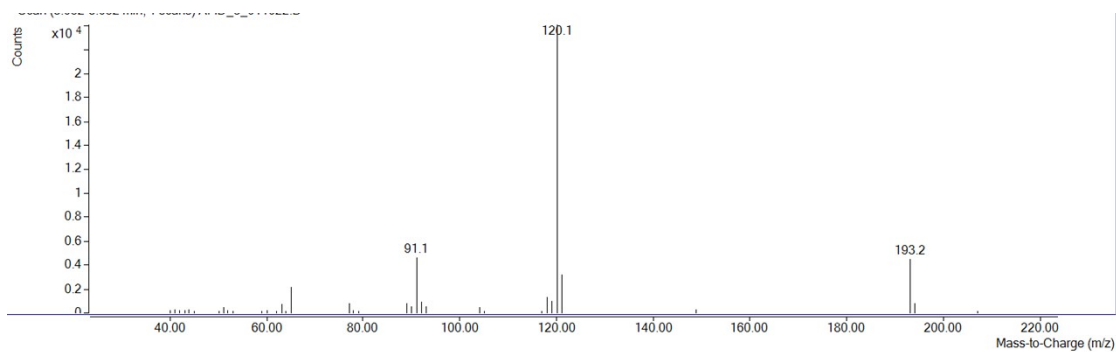
MS trace for monoalkylated product **3a** corresponding to figure S10



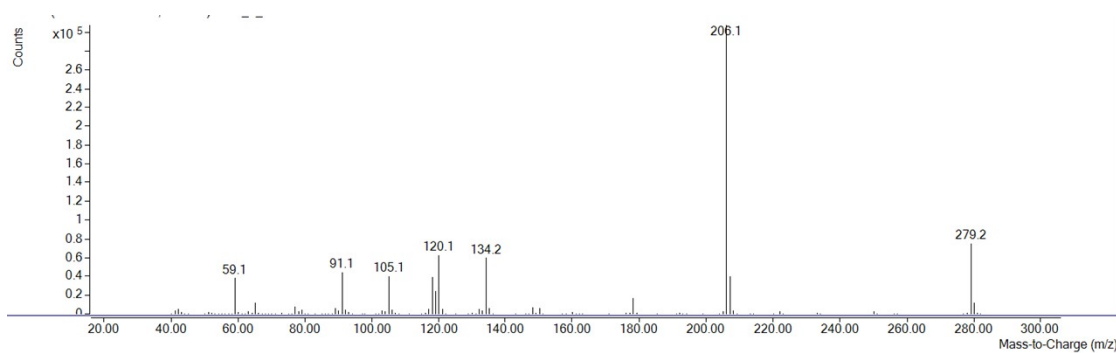
MS trace for dialkylated product corresponding to figure S10



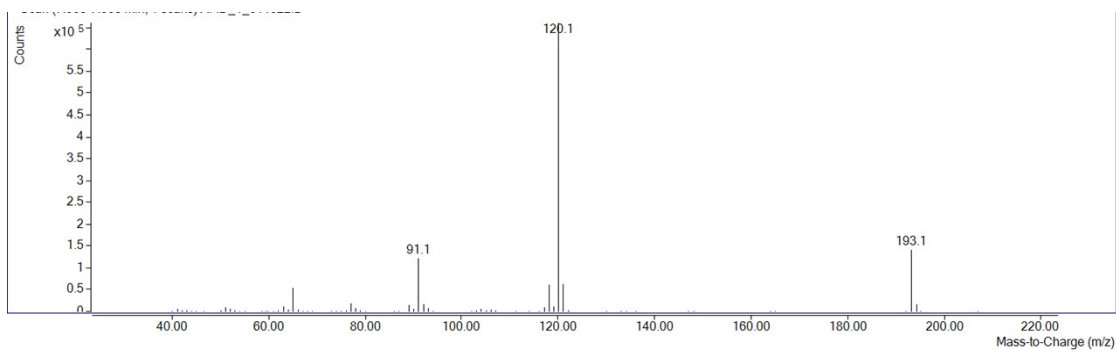
MS trace for monoalkylated product **3b** corresponding to figure S11



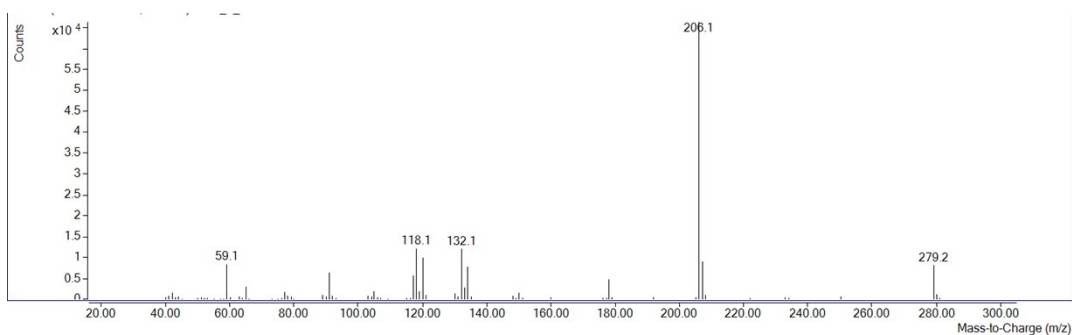
MS trace for dialkylated product corresponding to figure S11



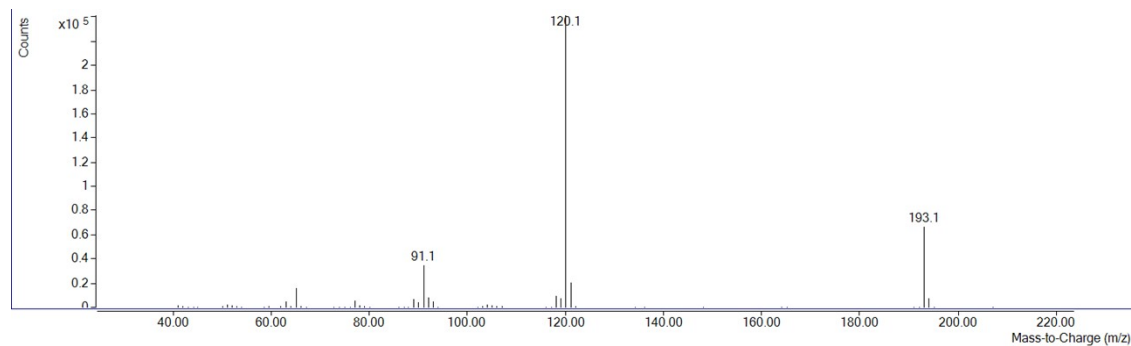
MS trace for monoalkylated product **3c** corresponding to figure S12



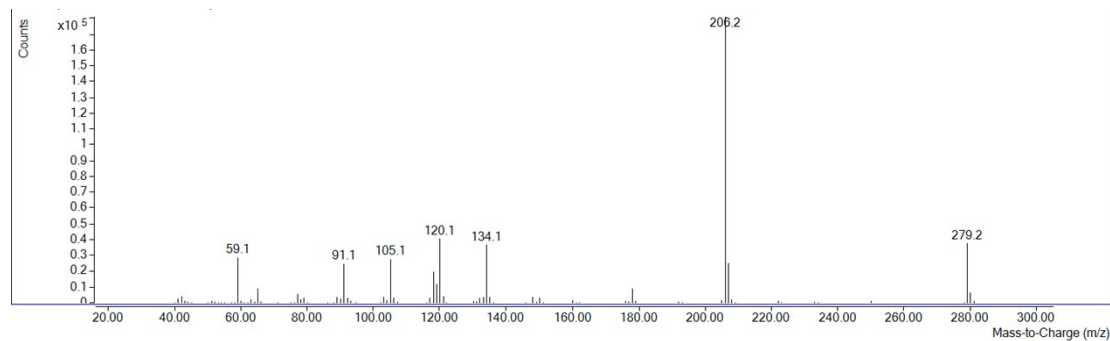
MS trace for dialkylated product corresponding to figure S12



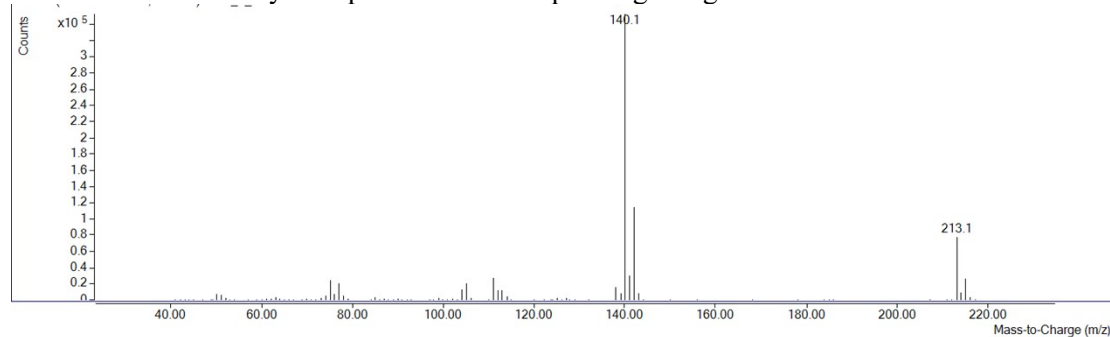
MS trace for monoalkylated product **3d** corresponding to figure S13



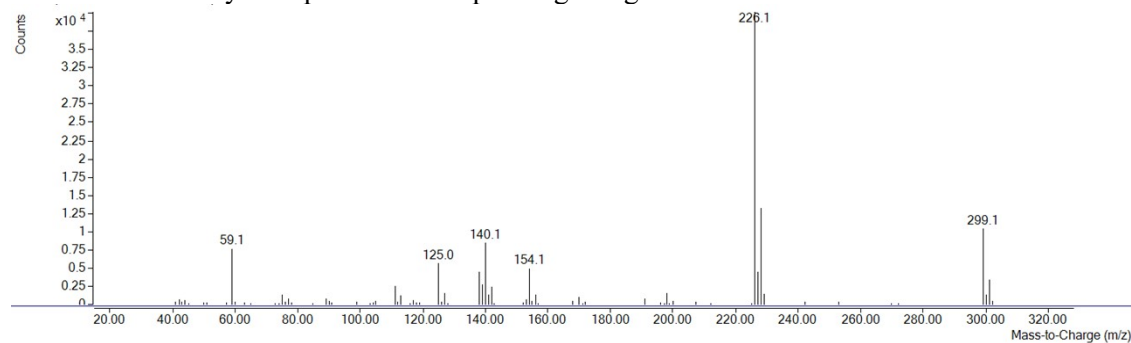
MS trace for dialkylated product corresponding to figure S13



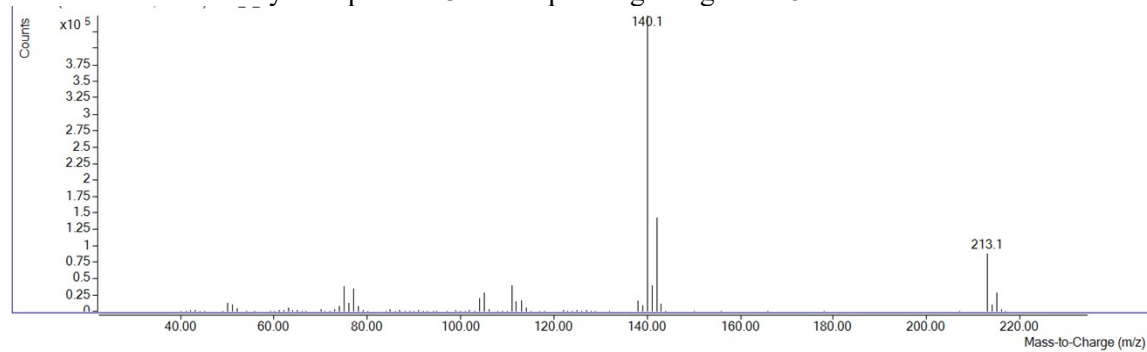
MS trace for monoalkylated product **3e** corresponding to figure S14



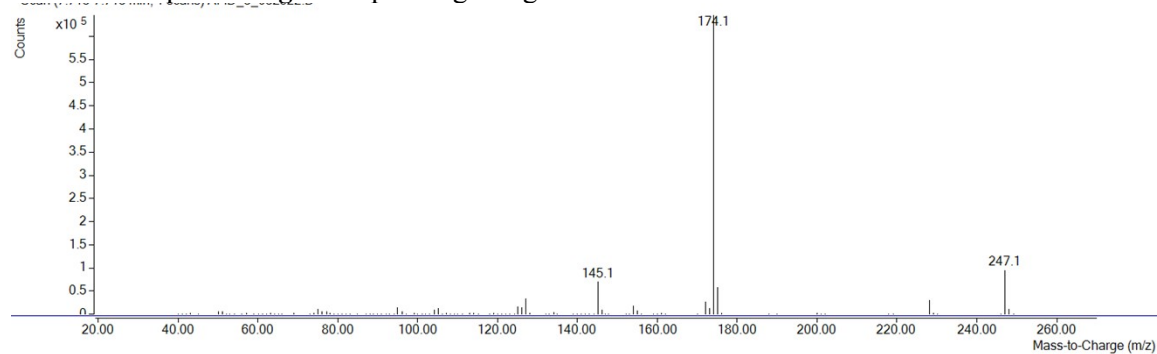
MS trace for dialkylated product corresponding to figure S14



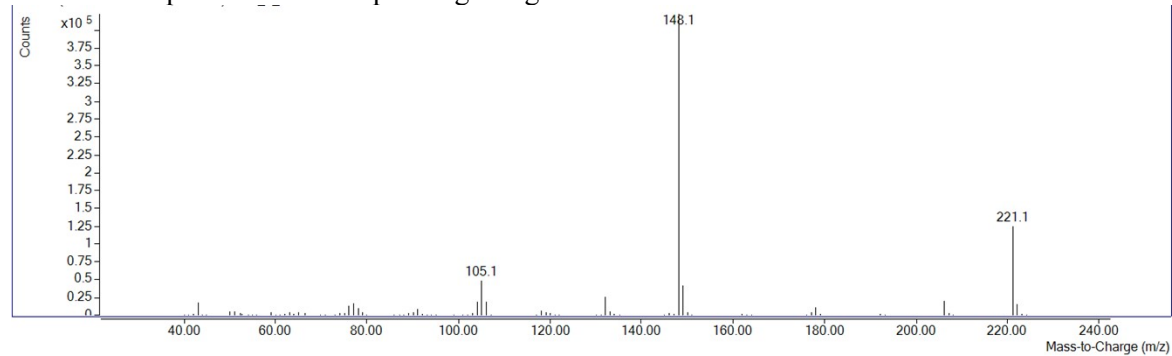
MS trace for monoalkylated product **3f** corresponding to figure S15



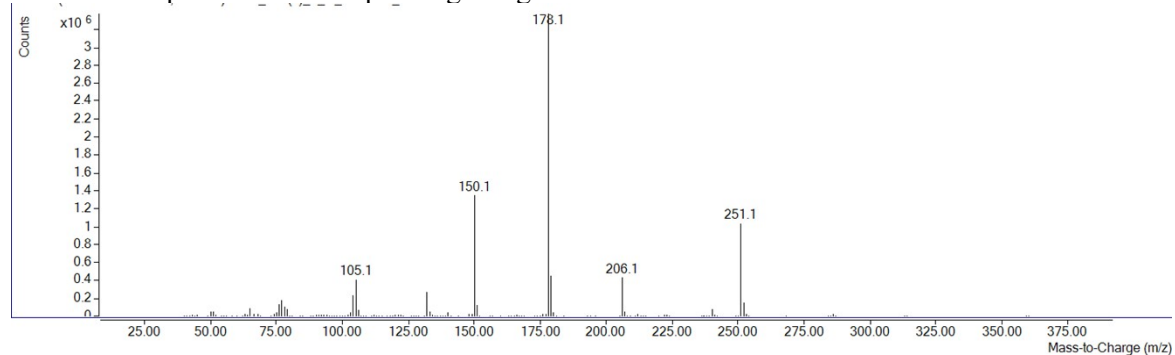
MS trace for product **3g** corresponding to figure S16



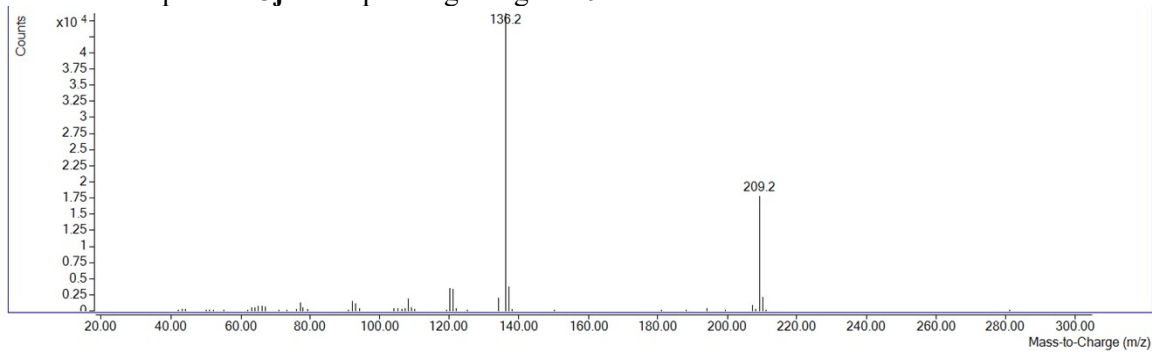
MS trace for product **3h** corresponding to figure S17



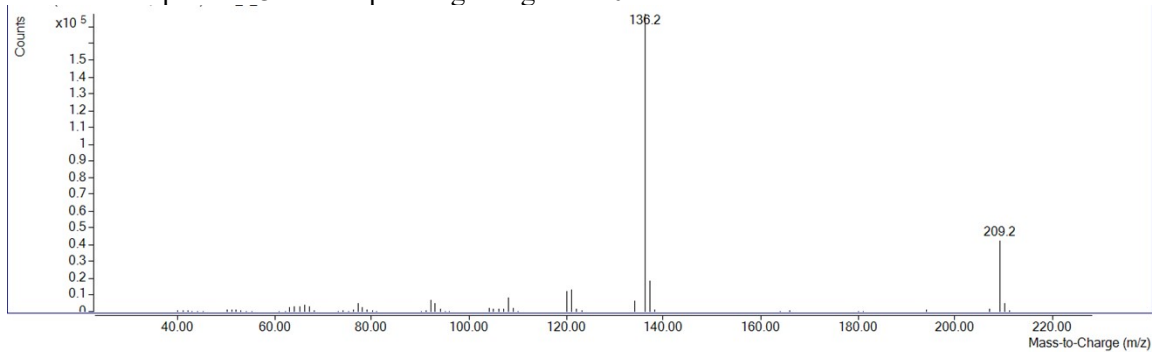
MS trace for product **3i** corresponding to figure S18



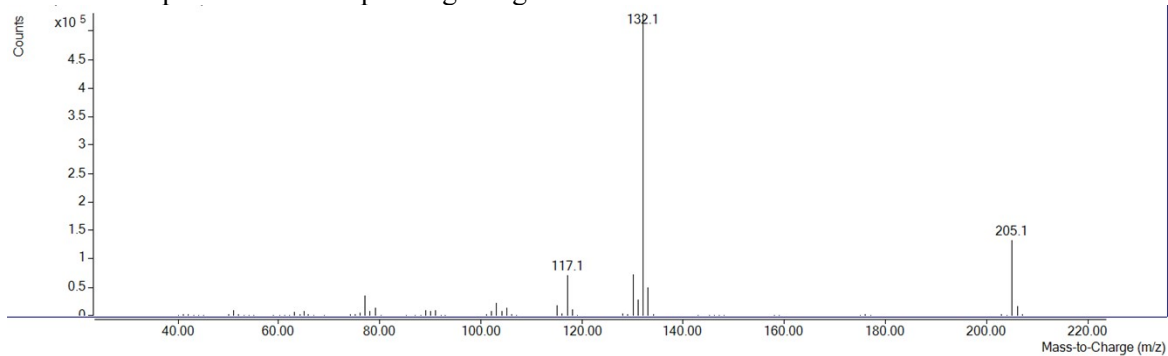
MS trace for product **3j** corresponding to figure 19



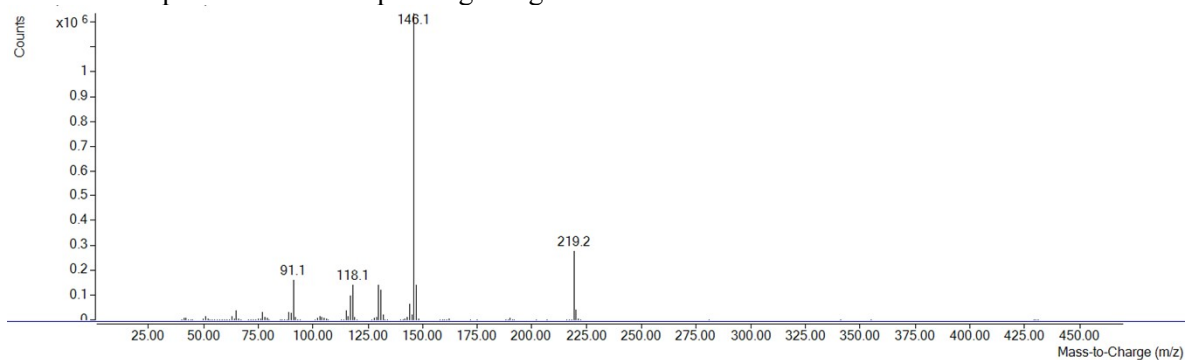
MS trace for product **3k** corresponding to figure S20



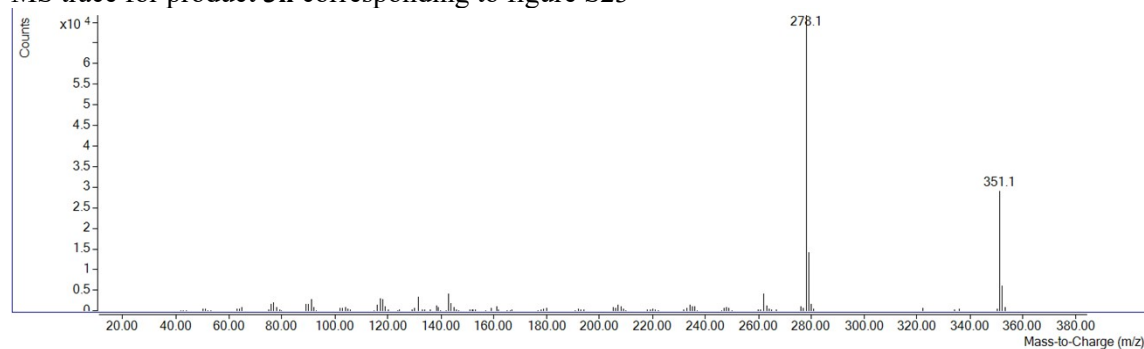
MS trace for product **3l** corresponding to figure S21



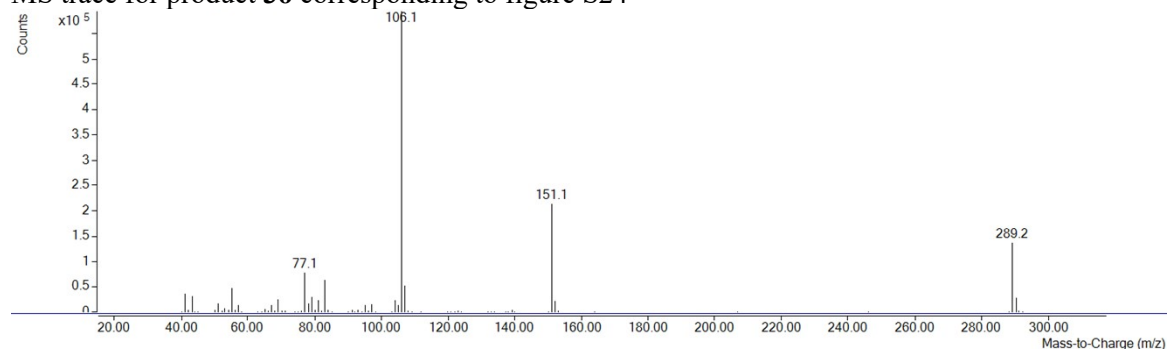
MS trace for product **3m** corresponding to figure S22



MS trace for product **3n** corresponding to figure S23



MS trace for product **3o** corresponding to figure S24



X. References

1. Grimm, C.; Lazzarotto, M.; Pompei, S.; Schichler, J.; Richter, N.; Farnberger, J. E.; Fuchs, M.; Kroutil, W., Oxygen-Free Regioselective Biocatalytic Demethylation of Methyl-phenyl Ethers via Methyltransfer Employing Veratrol-O-demethylase. *ACS Catalysis* **2020**, *10* (18), 10375-10380.
2. Datta, S.; Koutmos, M.; Patridge, K. A.; Ludwig, M. L.; Matthews, R. G., A disulfide-stabilized conformer of methionine synthase reveals an unexpected role for the histidine ligand of the cobalamin cofactor. *Proceedings of the National Academy of Sciences* **2008**, *105* (11), 4115-4120.
3. Heckman, K. L.; Pease, L. R., Gene splicing and mutagenesis by PCR-driven overlap extension. *Nature Protocols* 2007, *2* (4), 924-932.
4. Xinhang Yang, Benjamin H. R. Gerroll, Yuhua Jiang, Amardeep Kumar, Yasmine S. Zubi, Lane A. Baker, Jared C. Lewis; Controlling Non-Native Cobalamin Reactivity and Catalysis in the Transcription Factor CarH. *ACS Catalysis* **2022**, *12*, 935-942
5. Qiao, J.; Song, Z.-Q.; Huang, C.; Ci, R.-N.; Liu, Z.; Chen, B.; Tung, C.-H.; Wu, L.-Z. Direct, Site-Selective and Redox-Neutral α -C-H Bond Functionalization of Tetrahydrofurans via Quantum Dots Photocatalysis. *Angew. Chem. Int. Ed.* **2021**, *60* (52), 27201-27205.
6. Snodgrass HM, Mondal D, Lewis J. Directed Evolution of Flavin-Dependent Halogenases for Atroposelective Halogenation of 3-Aryl-4(3H)-quinazolinones via Kinetic or Dynamic Kinetic Resolution. *Chemrxiv* **2022**; <https://doi.org/10.26434/chemrxiv-2022-b3n3j>
7. Jost, M.; Fernandez-Zapata, J.; Polanco, M. C.; Ortiz-Guerrero, J. M.; Chen, P. Y.; Kang, G.; Padmanabhan, S.; Elias-Arnanz, M.; Drennan, C. L., Structural basis for gene regulation by a B12-dependent photoreceptor. *Nature* 2015, *526* (7574), 536-41.

